HHS Public Access

Author manuscript

J Neurochem. Author manuscript; available in PMC 2024 July 21.

Published in final edited form as:

J Neurochem. 2024 July ; 168(7): 1340–1358. doi:10.1111/jnc.16084.

Muscle-building supplement β-hydroxy β-methylbutyrate stimulates the maturation of oligodendroglial progenitor cells to oligodendrocytes

Malabendu Jana[1,2], **Shelby Prieto**[1], **Sukhamoy Gorai**[1], **Sridevi Dasarathy**[1], **Madhuchhanda Kundu**[1], **Kalipada Pahan**[1,2]

[1]Department of Neurological Sciences, Rush University Medical Center, Chicago, Illinois, USA

[2]Division of Research and Development, Jesse Brown Veterans Affairs Medical Center, Chicago, Illinois, USA

Abstract

Oligodendrocytes are the myelinating cells in the CNS and multiple sclerosis (MS) is a demyelinating disorder that is characterized by progressive loss of myelin. Although oligodendroglial progenitor cells (OPCs) should be differentiated into oligodendrocytes, for multiple reasons, OPCs fail to differentiate into oligodendrocytes in MS. Therefore, increasing the maturation of OPCs to oligodendrocytes may be of therapeutic benefit for MS. The β-hydroxy β-methylbutyrate (HMB) is a muscle-building supplement in humans and this study underlines the importance of HMB in stimulating the maturation of OPCs to oligodendrocytes. HMB treatment upregulated the expression of different maturation markers including PLP, MBP, and MOG in cultured OPCs. Double-label immunofluorescence followed by immunoblot analyses confirmed the upregulation of OPC maturation by HMB. While investigating mechanisms, we found that HMB increased the maturation of OPCs isolated from peroxisome proliferator-activated receptor $\beta^{-/-}$ (PPARβ$^{-/-}$) mice, but not PPARα$^{-/-}$ mice. Similarly, GW6471 (an antagonist of PPARα), but not GSK0660 (an antagonist of PPARβ), inhibited HMB-induced maturation of OPCs. GW9662, a specific inhibitor of PPARγ, also could not inhibit HMB-mediated stimulation of OPC maturation. Furthermore, PPARα agonist GW7647, but neither PPARβ agonist GW0742 nor PPARγ agonist GW1929, alone increased the maturation of OPCs. Finally, HMB treatment of OPCs led to the recruitment of PPARα, but neither PPARβ nor PPARγ, to the *PLP* gene promoter. These results suggest that HMB stimulates the maturation of OPCs via PPARα and that HMB may have therapeutic prospects in remyelination.

Correspondence Kalipada Pahan, Department of, Neurological Sciences, Rush University, Medical Center, 1735 West Harrison St, Suite 310, Chicago, IL 60612, USA. kalipada_pahan@rush.edu.

AUTHOR CONTRIBUTIONS

Malabendu Jana: Data curation; formal analysis; investigation; methodology; validation; visualization. **Shelby Prieto:** Data curation; formal analysis; investigation; visualization. **Sukhamoy Gorai:** Data curation; formal analysis; investigation; visualization. **Sridevi Dasarathy:** Data curation; formal analysis; investigation; visualization. **Madhuchhanda Kundu:** Formal analysis; investigation; visualization. **Kalipada Pahan:** Conceptualization; funding acquisition; project administration; resources; supervision; writing – original draft; writing – review and editing.

CONFLICT OF INTEREST STATEMENT

The authors declare no conflict of interest.

SUPPORTING INFORMATION

Additional supporting information can be found online in the Supporting Information section at the end of this article.

Keywords

differentiation; HMB; myelination; oligodendroglial progenitor cells; PPAR

1 | INTRODUCTION

Myelin is a lipid-rich plasma membrane (Hartline, 2008; Smith, 1921) that creates manifold concentric coatings around the axon to preserve the conduction of electrical impulses through a healthy neuron (Sanders & Whitteridge, 1946). During demyelination, the ionic conduction through the neuron is reduced, ultimately leading to axonal loss. Therefore, demyelination is assumed as an important pathological hallmark in many neuroinflammatory diseases including multiple sclerosis (MS) (Friese et al., 2014), Devic's disease (Jarius & Wildemann, 2019), progressive multifocal leukoencephalopathy (PML) (Richardson, 1961), Krabbe disease (Kondo et al., 2011), and X-Adrenoleukodystrophy (X-ALD) (Pahan et al., 1998; Zhu et al., 2020). Since oligodendrocytes are the only myelin-synthesizing cells in the CNS, the death or dysfunction of oligodendrocytes is considered as the major cause of demyelination (Akassoglou et al., 1998; Caprariello et al., 2012; Jana et al., 2009; Jana & Pahan, 2013; Kondo et al., 2011; Singh et al., 1998; Traka et al., 2016). Although oligodendroglial progenitor cells (OPCs) should be differentiated into mature oligodendrocytes for remyelination of an injured CNS, the failure of OPCs to differentiate into oligodendrocytes in a demyelinating CNS coupled with widespread neuroinflammation is a major therapeutic challenge to recover myelin in demyelinated brains (Kirby et al., 2019; Kuhn et al., 2019; Tepavcevic & Lubetzki, 2022). Therefore, understanding the mechanisms by which OPCs are differentiated into mature oligodendrocytes and the identification of nontoxic compounds/drugs for the stimulation of OPC differentiation are important areas of research.

The β-hydroxy β-methylbutyrate (HMB) is present in local GNC stores as a body-building supplement. Accordingly, bodybuilders regularly use HMB to increase exercise-induced gains in muscle size and muscle strength and improve exercise performance. HMB treatment also increases aerobic and anaerobic capacity among combat sports athletes. In addition, in a 12-week randomized, double-blind, placebo-controlled crossover study among 42 highly-trained combat sports athletes (Durkalec-Michalski et al., 2017), HMB treatment leads to an increase in fat-free mass with a simultaneous decrease in fat mass. Even after long-term use, HMB does not exhibit any side effects. Therefore, HMB is considered as a safe supplement in humans. Recently we have seen that HMB stimulates hippocampal plasticity in an animal model of Alzheimer's disease (Paidi, Raha, et al., 2023) and protects mice from experimental autoimmune encephalomyelitis (EAE), an animal model of MS (Sheinin et al., 2023). Here, we demonstrated that HMB was capable of stimulating the maturation of OPCs into oligodendrocytes. Interestingly, HMB required PPARα, but neither PPARβ nor PPARγ, to stimulate the differentiation of OPCs into oligodendrocytes. These results suggest that HMB may be repurposed for remyelination.

2 | MATERIALS AND METHODS

2.1 | Reagents

HMB (catalog number: 55453) was purchased from Millipore-Sigma (Burlington, MA). GW9662 (catalog number: sc202641) was purchased from Santa Cruz Biotechnology (Dallas, TX). Molecular Biology grade agarose (catalog number: 1613102) was purchased from Bio-Rad (Hercules, CA). DMEM/F-12 (catalog number: 10–092-CV), Hanks' balanced salt solution (catalog number: 21–022-CM), L-glutamine (catalog number: 25–005-CI), 0.05% trypsin (catalog number: 25–051-CI), and antibiotic/antimycotic (catalog number: 30–004-CI) were obtained from ThermoFisher (Waltham, MA). Fetal bovine serum or FBS (catalog number: EF-0500-A) was obtained from Atlas Biologicals (Fort Collins, CO). Alexa Fluor 488 donkey anti-goat (RRID:AB_2340430), Alexa Fluor 647 donkey anti-rabbit (RRID:AB_2492288), and Alexa Fluor 488 donkey anti-mouse (RRID:AB_2340846) secondary antibodies used in immunostaining were obtained from Jackson ImmunoResearch (West Grove, PA).

2.2 | Animals

Animal maintenance and experiments were in accordance with National Institute of Health guidelines and were approved (protocol ID: 20-007) by the Institutional Animal Care and Use Committee of the Rush University of Medical Center, Chicago, IL. Mice were housed in ventilated micro-isolator cages in an environmentally controlled vivarium (7:00 a.m./7:00 p.m. light cycle; temperature maintained at 21–23°C; humidity 35%–55%). Animals were provided standard mouse chow and water ad libitum and closely monitored for health and overall well-being daily by veterinary staff and the investigator. This study was not preregistered.

PPARα$^{-/-}$ mice (RRID:IMSR_JAX:008154) and C57BL/6J (RRID:IMSR_JAX:000664) mice were obtained from Jackson Laboratory, Bar Harbor, ME, USA. PPARβ/δ$^{-/-}$“ mice (Shan et al., 2008) were kindly provided by Dr. Frank Gonzalez (NCI, NIH). These mice were maintained through genotyping as described by us (Chandra et al., 2018; Corbett et al., 2015; Patel et al., 2020).

2.3 | Isolation of mouse OPCs

OPCs were isolated from P1-P2 neonatal pups as described before (Dincman et al., 2012; Jana et al., 2007, 2012) with modifications. Briefly, the brain tissues from the pups were pooled together and placed together in the DMEM/F-12 media supplemented with 10% heat-inactivated fetal bovine serum. Cells were dissociated by trituration and single cell suspension was plated in poly-D-lysine pre-coated flasks containing complete DMEM/F12 media. On the 9th day, flasks were shaken for 2 h at 240 rpm to remove microglia from the rest of the cells. Then, on the 11th day, flasks were shaken overnight at 180 rpm, followed by 2 h of shaking at 240 rpm to isolate OPCs. In order to remove microglia and astrocytes from OPCs, suspended cells were allowed to adhere to uncoated flasks for 1 h. Non-adherent cells were centrifuged at 1000 rpm for 10 min and plated on experimental wells, plates, or coverslips in the presence of OPC medium [DMEM containing 4 mM L-glutamine (catalog number: G8540-10MG; Sigma), 1 mM sodium pyruvate (catalog number: P4562-25G;

Sigma), 0.1% BSA (catalog number: A9418-5G; Sigma), 50μg/mL apo-transferrin (catalog number: T2036-100MG; Sigma), 5μg/mL insulin (catalog number: H0888-1G; Sigma), 30 nM sodium selenite, 10 nM D-biotin, 1O nM hydrocortisone (catalog number: H0888-1G; Sigma), 10 ng/mL PDGF (catalog number: P3326; Sigma), and 10 ng/mL bFGF (catalog number: F0291; Sigma)]. During treatment, OPCs were cultured in an OPC medium in the absence of PDGF and bFGF and treated with different concentrations of HMB for different time periods as mentioned for particular experiments.

We used a total of 144 P1-P2 WT, 48 P1-P2 PPARα$^{-/-}$, and 48 P1-P2 PPARβ$^{-/-}$ neonatal pups for the isolation of OPCs in this study. Since on average, one pregnant mouse delivered 6 pups, we used 24 WT, 8 PPARα$^{-/-}$, and 8 PPARβ$^{-/-}$ pregnant mice for this study.

2.4 | Induction of experimental autoimmune encephalomyelitis (EAE)

C57BL/6 mice (8–10-weeks-old male) were immunized s.c. with 100 μg of MOG35-55 (catalog number: M4939-1 MG; Sigma) and 60 μg *M. tuberculosis* (catalog number: P7208; Sigma) in IFA. as described (Mondal et al., 2017, 2020; Mondal & Pahan, 2015). Mice also received two doses of pertussis toxin (150 ng/mouse) on 0 and 2 dpi (Mondal et al., 2012; Mondal & Pahan, 2015). Animal maintenance and experimental protocols were approved by the Rush University Medical Center. Animals were observed daily for clinical symptoms as described (Brahmachari & Pahan, 2007; Dasgupta et al., 2003, 2004; Mondal et al., 2009, 2018, 2020). Experimental animals were scored by a masked investigator, as follows: 0, no clinical disease; 0.5, piloerection; 1, tail weakness; 1.5, tail paralysis; 2, hind limb weakness; 3, hind limb paralysis; 3.5, forelimb weakness; 4, forelimb paralysis; 5, moribund or death.

Animals exhibiting hind limbs and limb paralysis were fed and watered through animal feeding needles. However, if any mouse came to the moribund stage, it was decapitated after anesthesia with ketamine/xylazine injectable because this combination is relatively safe in mice to achieve effective analgesia, muscle relaxation, and sedation. Mice were injected with ketamine (100 mg/kg body wt) and xylazine (5–7 mg/kg body wt) intraperitoneally. Conditions for moribund were as follows: Central nervous system disturbance (Head tilt, Seizures, Tremors, Circling, Spasticity, and Paresis); Inability to remain upright; Evidence of muscle atrophy; Chronic diarrhea or constipation; Rough coat and distended abdomen; Spreading area of alopecia caused by disease; Coughing, rales, wheezing and nasal discharge; Distinct jaundice and/or paleness (anemia); Markedly discolored urine, polyuria or anuria; Frank bleeding from any orifice; Persistent self-induced trauma.

2.4.1 | Treatment with EAE mice HMB—HMB was solubilized in 0.1% methylcellulose, and EAE mice were treated with HMB (5 mg/kg body wt) once daily in a volume of 50μL via gavage using gavage needle (Sheinin et al., 2023) starting from 10-day post-immunization (dpi), the onset of the disease. Therefore, control EAE mice received only 50 μL 0.1% methyl cellulose as vehicle via gavage. Treatment started daily at 10 AM (central time) and continued for 10 days.

During treatment, no mouse reached the moribund stage (conditions are described above) or died. After 10 days of treatment, mice were anesthetized with ketamine/xylazine injectables followed by perfusion with PBS and paraformaldehyde. During perfusion, animals died.

For Figure S3, 5 male C57/BL6 mice (8–10-weeks-old male) were used in each group. Therefore, 15 male C57/BL6 mice were used for three groups. No randomization was performed to allocate subjects in the study.

2.5 | In silico molecular docking study

It was performed as described earlier (Paidi, Jana, et al., 2023; Roy et al., 2015, 2016) with modifications. Briefly, to understand how HMB interacts with the PPARs, we first generated in silico model structure of unavailable crystal structures of PPARα, PPARβ, and PPARγ. The homology models of PPARα, PPARβ, and PPARγ were built with the Swiss model, an automated online server using the sequences (NCBI ID NP_001106889.1 [aa 196-468], NP_035275.1 [aa 172-440], and NP_001295283.1 [aa 205-471], respectively) available on the NCBI website. The target template was uploaded and searched for the most identical homologous sequence. The sequence identity between the two sequences NP_001106889.1 and 3sp6.1.A was 92%, NP_035275.1 and 5u42.2 and NP_001295283.1 and 3e00.1.B was 98%. Finally, the model was obtained by blasting the target sequence with the most identical homologous sequence. The quality of the model structures was further verified. Autodock4 (The Scripps Research Institute, La Jolla, USA) tool was used to dock the crystal structure of PPARβ (PDB ID: 2j14), PPARα, and PPARγ homology models. Following grid parameters were used to cover the entire protein- PPARα (X = 113, Y = 113, Z = 113, center: x = 9.096, y = 0.075, z = 24.947 and spacing: 0.375), PPARβ (X = 113, Y = 113, Z = 113, center: x = 2.956, y = 0.507, z = 3.116 and spacing: 0.375) and PPARγ (X = 111, Y = 111, Z = 111, center: x = 31.337, y = −9.998, z = 35.524 and spacing: 0.375). All parameters were set to default for running the docking. Finally, the minimum energy dock structure was chosen as the best docking pose. PyMOL software (The PyMol Molecular Graphics System, Version 2.0, Schrödinger, LLC.) was used to create the final representable image.

2.6 | Semi-quantitative RT-PCR analysis

Semi-quantitative RT-PCR was carried out as described earlier (Ghosh et al., 2007, 2009). To remove any contaminating genomic DNA, total RNA was digested with Invitrogen™ DNase (catalog number: 18047019; ThermoFisher Scientific), and 1 μg of total RNA was reverse transcribed using oligo$(dT)_{12-18}$ (catalog number: 18418012; ThermoFisher Scientific) as a primer and Promega MMLV reverse transcriptase (catalog number: PR-M1701; ThermoFisher Scientific) in a 20 μL reaction mixture as follows: cDNA synthesis at 50°C for 30 min; reverse transcriptase inactivation at 95°C for 10 min. The resulting cDNA was appropriately diluted, and diluted cDNA was amplified for 38 cycles (denaturation of templates at 95°C for 30 s, annealing of primers at 52°C for 45 s, initial extension of primers at 72°C for 2 min, and final extension of primers at 72°C for 10 min) using Promega PCR master mix (catalog number: PRM7505; ThermoFisher Scientific) and following primers.

MBP (mouse)	Sense: 5′-TGGAGAGATTCACCGAGGAGAGGC-3′
	Antisense: 5′-TGGAGAGATTCACCGAGGAGAGGC-3′
PLP (mouse)	Sense: 5′-CTTCCCTGGTGGCCACTGGATTGT-3′

	Antisense: 5′-CCGCAGATGGTGGTCTTGTAGTCG-3′
MOG (mouse)	Sense: 5′-CCTCTCCCTTCTCCTCCTTC-3′
	Antisense: 5′-AGAGTCAGCACACCGGGGTT-3′
CNPase (mouse)	Sense: 5′-CTACCCTCCACGAGTGCAAGACGCT-3′
	Antisense: 5′-AGTCTAGTCGCCACGCTGTCTTGGG-3′
NG2 (mouse)	Sense: 5′-TTCCTTCGCCTTACAAGTCC-3′
	Antisense: 5′-CTCACTCACCAGGAGCTGTAG-3′
GAPDH (mouse)	Sense: 5′-CAGGGGATGATCATGGCTTCTCC-3′
	Antisense: 5′-GATGCTCACAAGAGCCCCGTTAGC-3′

Amplified products were electrophoresed on a 1.8% agarose gels and visualized by ethidium bromide (catalog number: 15-585-011; ThermoFisher Scientific) staining.

2.7 | Real-time PCR analysis

It was performed using the ABI-Prism7700 sequence detection system (Applied Biosystems) as described earlier (Dutta et al., 2022; Jana, Dutta, et al., 2023). The mRNA expressions of respective genes were normalized to the level of GAPDH mRNA. Data were processed by the ABI Sequence Detection System 1.6 software and analyzed by ANOVA.

2.8 | Western blot

It was performed as described before (Dutta et al., 2021; Mondal et al., 2020; Paidi et al., 2021). For whole cell lysates, samples were homogenized in RIPA buffer (catalog number: AAJ62524AE; ThermoFisher Scientific) containing protease and phosphatase inhibitors (catalog number: PPC1010-1ML; Sigma), rotated end over end for 30 min at 4°C and centrifuged for 10 min at 15000g. The supernatant was aliquotted and stored at −80°C until use. Protein concentrations were determined using a NanoDrop 2000 (ThermoFisher Scientific), and 20–30 μg sample was heat-denatured and resolved on 10% or 12% polyacrylamide-SDS gels in MES buffer or 1X SDS running buffer. Proteins were transferred to 0.45 μm nitrocellulose membranes under wet conditions. Membranes were blocked for 1 h with Li-Cor blocking buffer, incubated with primary antibodies (Table S1) overnight at 4°C under shaking conditions, washed, incubated with IR-dye labeled secondary antibodies at room temperature, washed and visualized with the Odyssey Infrared Imaging System (Li-Cor Biosciences). Blots were converted to binary, analyzed using ImageJ (NIH), and normalized to the loading control (β-actin).

2.9 | Luciferase assay

It was performed as described previously (Pahan et al., 2000, 2002). Briefly, cells plated at 60%−70% confluency were transfected with tk-PPREx3-Luc, a PPRE-dependent luciferase reporter construct, using Lipofectamine LTX Reagent with PLUS Reagent (catalog number: A12621; ThermoFisher Scientific). Following 24 h of transfection, cells were exposed to different concentrations of HMB under serum-free conditions for 2 h. Luciferase activities were analyzed in cell extracts using the Luciferase Assay System kit (catalog number: E1501; Promega) in a TD-20/20 Luminometer (Turner Designs).

2.10 | Immunostaining

Cells were washed three times with 1X PBS, fixed in 4% paraformaldehyde for 10 min or with chilled methanol (catalog number: A412-500; ThermoFisher) overnight, washed again with 1X PBS and incubated first with primary antibodies (Table S1) followed by Alexa Fluor 488- or Alexa Fluor 647-conjugated AffinityPure Donkey secondary antibodies (Jackson ImmunoResearch) as described earlier (Gottschalk et al., 2021; Kundu et al., 2017). After secondary antibody incubation, coverslips were rinsed in 1X PBS, mounted on slides in Fluoromount (catalog number: F4680; Sigma), and imaged using an Olympus BX41 fluorescent microscope equipped with a Hamamatsu ORCA-03G camera. Immunostaining of tissue was performed by fixing the brains in 4% paraformaldehyde followed by 30% sucrose. Tissue was sectioned every 40 microns on a Leica Crysotat CM3050 S and kept in cryoprotectant. DAPI was added at the final step of washing of secondary antibodies for staining nuclei.

3 | CELL COUNTING

Counting analysis was performed using the Olympus microsuite V software with the help of touch counting module as described (Chandra et al., 2017). After acquiring images under a 20 × objective lens, images were further analyzed as follows. Before counting cells, the entire Image area was calibrated with the help of a rectangular box available in the touch counting panel. Once the area of the image was measured, touch counting program was applied to count number of fluorescent signals. Next, the total number of signals in a given area was divided by the total area of the image and presented as number of cells per square millimeter unit.

3.1 Chromatin immunoprecipitation (ChIP) assay

Recruitment of PPARs to the *PLP* gene promoter was determined by ChIP assay as described earlier (Jana et al., 2013; Jana, Dasarathy, et al., 2023; Kundu et al., 2016). Briefly, OPCs were treated with different concentrations of HMB for 1 h in the absence of FGF and PDGF. Cells were fixed by adding formaldehyde (1% final concentration), and cross-linked adducts were resuspended and sonicated. ChIP was performed on the cell lysate by overnight incubation at 4°C with 2 μg of anti-PPARα, anti-PPARβ, anti-PPARγ, anti-CBP, or anti-RNA Polymerase II antibodies followed by incubation with protein G agarose (Santa Cruz Biotechnology) for 2 h. The beads were washed and incubated with elution buffer. To reverse the cross-linking and purify the DNA, precipitates were incubated in a 65°C incubator overnight and digested with proteinase K. DNA samples were then purified, precipitated, and precipitates were washed with 75% ethanol, air-dried, and resuspended in TE buffer. The following primers were used for the amplification of chromatin fragments of mouse *PLP* gene.

Sense: 5′-GAGGAGAGGAGGAGGGAAACGAGCC-3′.

Antisense: 5′-GCGGCTGACTTTGCTCAGCTGGAAG-3′.

3.2 | Blinding and statistical analysis

All Western blot, RT-PCR, real-time PCR, and immunohistochemical analyses were performed in a blinded manner. Laboratory personnel only knew about ID of each sample. For animal experiments, five mice were included in each group. All cell culture experiments were repeated at least three times. There is no restriction on the availability of data. The D'Agostino-Pearson test (GraphPad Prism 10 software) was used for normality. Statistical analyses were performed with one-way ANOVA with dose as a single factor. Descriptive statistics of one-way ANOVA were included in figure legends with pertinent F values. While analyzing the significance between the two groups, a paired t-test was performed. Results were statistically analyzed using GraphPad Prism 10.1.1. Values are expressed as either mean±SD or mean±SEM. One-way AN OVA followed by Tukey's multiple comparisons was performed for statistical analyses among multiple groups. The criterion for statistical significance was $p<0.05$. No test for outliers was conducted on the data. The sample size was similar to those reported in previous publications (Corbett et al., 2015; Rangasamy et al., 2015) and is mentioned in figure legends.

4 | RESULTS

4.1 | Effect of HMB on the maturation of OPCs into oligodendrocytes

During remyelination, new myelinating oligodendrocytes are generated from OPCs. NG2, a type-1 membrane protein, is present only in OPCs, and is known to stimulate proliferation of OPC via increasing growth factor signaling (Sakry & Trotter, 2016). Similarly, A2B5, a cell surface ganglioside epitope, is expressed in OPCs probably to increase the self-renewal property of these cells (Figarella-Branger et al., 2022). Therefore, NG2 and A2B5 are considered reliable markers of OPCs. Accordingly, the reduction of these markers along with subsequent induction of oligodendrocyte markers such as MBP and PLP are used to monitor the generation of oligodendrocytes from OPCs. Therefore, we examined the effect of HMB, a popular body-building drug, on the maturation of OPCs.

Primary mouse OPCs isolated from WT mice were treated with different doses (0.25, 0.5, 1, 2, 5, and 10 μM) of HMB for 5 h followed by real-time PCR to monitor the mRNA expression of PLP (Figure S1A) and MBP (Figure S1B). Even at the lowest dose (0.25 μM) of HMB used in this study, we observed a significant ($p<0.05$) increase in mRNA expression of PLP (Figure S1A) and MBP (Figure S1B). However, the fold induction increased gradually with higher doses reaching almost a plateau at 2, 5, and 10 μM HMB (Figure S1A,B). Therefore, in further experiments with OPCs, we used 2, 5, and/or 10 μM HMB. WT OPCs, after 24 h of treatment with HMB, were immunostained with PLP and A2B5 (Figure 1a). We found that HMB upregulated the level of PLP with strong inhibition of A2B5 (Figure 1a). Similarly, double-labeling with MBP and NG2 revealed a prominent decrease in NG2 with a strong increase in MBP (Figure 1b). To confirm the finding further, we performed cell counting that clearly showed a marked reduction in $A2B5^+$ (Figure 1c) and $NG2^+$ (Figure 1d) cells along with a strong increase in PLP^+ (Figure 1e) and MBP^+ (Figure 1f) cells.

In addition to MBP and PLP, oligodendrocytes also express 2′,3′-cyclic nucleotide 3′-phosphodiesterase (CNPase) and myelin oligodendrocyte glycoprotein (MOG). Therefore, we also examined the effect of HMB on the mRNA expression of different myelin-specific genes including CNPase and MOG in OPCs. As evident from Figure 2a, HMB treatment strongly upregulated the mRNA expression of MBP, PLP, CNPase, and MOG in OPCs. A significant increase in mRNA expression of MBP, PLP, CNPase, and MOG was observed even at a concentration of 2 μM HMB (Figure 2a). Real-time PCR results also corroborated the increase in myelin-specific molecules by HMB (MBP, Figure 2b; PLP, Figure 2c; CNPase, Figure 2d; MOG, Figure 2e). However, consistent with immunostaining results, we found a decrease in mRNA expression of NG2 by HMB treatment (RT-PCR, Figure 2a; real-time PCR, Figure 2f). To further confirm the upregulation of myelin-specific molecules by HMB, we performed Western blot analysis that also showed upregulation of the protein level of MBP (Figure 2g,h), PLP (Figure 2g,i) and MOG (Figure 2g,j) in OPCs by HMB treatment.

4.2 | HMB interacts with PPARα and PPARβ, but not PPARγ

Since HMB stimulated the differentiation of OPCs to oligodendroglia, we were prompted to investigate underlying mechanisms. Earlier we have demonstrated that different PPARs are present in pre-oligodendrocytes and that PPARβ plays an important role in gemfibrozil-mediated upregulation of myelin-specific genes (Jana et al., 2012). Recently we have seen that HMB stimulates hippocampal plasticity via PPARα (Paidi, Raha, et al., 2023) and protects mice from EAE via PPARβ (Sheinin et al., 2023). Therefore, here, we examined the role of all three PPARs. We used SwissDock, a rigid body protein-ligand docking tool, to search the interaction between HMB and different PPARs. Since all three PPARs harbor well-defined ligand-binding domain (LBD) where different ligands bind for the activation of PPARs, we focused on the LBD. Ligand-binding pocket of PPARα is identified by S280, Y314, and Y464 (Patel et al., 2018; Roy et al., 2015). While gemfibrozil binds to the Y464 residue, aspirin interacts with the Y314 residue (Patel et al., 2018; Roy et al., 2015). We observed that HMB docked nicely in the LBD of PPARα (Figure 3a) and PPARβ (Figure 3b), but not PPARγ (Figure 3c). Although for PPARα LBD, HMB displayed H-bonding with H440, Y464, Y314, and S280, the strongest H-bonding (1.7 Å) was observed with S280 (Figure 3d). To understand the importance of this binding, S280 was mutated to A280 followed by performing in silico analysis to examine the interaction between HMB and S280A PPARα. Interestingly, HMB could not enter into the ligand-binding pocket of PPARα S280A (Figure S2A,B), indicating the importance of S280 of PPARα LBD in facilitating the binding of HMB. On the contrary, HMB formed H-bonding with H413, Y437, H287, and T253 residues of PPARβ LBD (Figure 3e). In contrast, HMB interacted with PPARγ nonspecifically on the surface of the protein (Figure 3f).

4.3 | Activation PPARα in OPCs and astrocytes by HMB

Since PPARs are nuclear hormone receptors that need a ligand for nuclear translocation, we monitored the nuclear translocation of PPARα and PPARβ in OPCs in response to HMB. As expected, both PPARα (Figure 4a) and PPAR 暻 (Figure 4b) are present in cytoplasm and perinuclear space of control OPCs. However, 1 h treatment of OPCs with HMB led to nuclear translocation of PPARα (Figure 4a; red arrow). On the contrary, after HMB

treatment, PPARβ remained in the cytoplasm of OPCs (Figure 4b; red arrowhead). This finding was further confirmed by MFI quantification of nuclear PPARα and PPARβ in OPCs (Figure 4c). These results suggest that although OPCs are rich in both PPARα and PPARβ, HMB treatment induces nuclear translocation of PPARα, but not PPARβ, in OPCs.

Next, we monitored the activation of PPAR using the PPRE-driven reporter activity in astrocytes isolated from WT, PPARα$^{-/-}$ and PPARβ$^{-/-}$ mice because astrocytes are easier to transfect than OPCs. HMB treatment significantly increased PPRE-driven luciferase activity in WT astrocytes (Figure 4d), indicating the activation of PPAR by HMB in astrocytes. However, HMB remained unable to induce PPRE-motivated luciferase activity in PPARα$^{-/-}$ astrocytes (Figure 4e). In contrast, marked upregulation of PPRE-inspired luciferase activity was found in PPARβ$^{-/-}$ astrocytes (Figure 4f). To prove the role of PPARα further, PPARα$^{-/-}$ astrocytes were transfected with full-length *PPARα* plasmid followed by treatment with HMB. Upregulation of PPRE-driven luciferase activity by HMB (Figure 4g) in PPARα$^{-/-}$ astrocytes transfected with full-length *PPARα*, but not empty vector *pcDNA3*, clearly indicates an important role of PPARα in the activation in PPRE in astrocytes.

Since PPARγ$^{-/-}$ mice die in the fetus, to investigate the role of PPARγ in HMB-mediated upregulation of PPRE-driven luciferase, we employed GW9662, a specific inhibitor of PPARγ. However, GW9662 could not inhibit HMB-induced activation of PPRE-luciferase in WT astrocytes (Figure 4h). These results suggest the involvement of PPARα, but neither PPARβ nor PPARγ, in HMB-induced upregulation on PPRE-luciferase activity in astrocytes. Moreover, although in silico results indicated docking of HMB to the LBD of both PPARα and PPARβ, HMB induced the activation of PPARα, but not PPARβ, in primary mouse astrocytes and OPCs.

4.4 | HMB requires PPARα, but neither PPARβ nor PPARγ, to stimulate the maturation of OPCs into oligodendrocytes

Next, we examined the involvement of PPARα, PPARβ, and PPARγ in the HMB-mediated maturation of OPCs into oligodendrocytes. OPCs isolated from PPARα$^{-/-}$ and PPARβ$^{-/-}$ mice were treated with different concentrations of HMB. Although HMB treatment upregulated the level of PLP with strong inhibition of A2B5 in WT OPCs (Figure 1a), HMB remained unable to decrease A2B5 and increase PLP in PPARα$^{-/-}$ OPCs (Figure 5a), indicating that HMB needs PPARα to stimulate the maturation of OPCs. This was confirmed by quantification of PLP^{+} (Figure 5c) and A2B5^{+} (Figure 5d) cells. In contrast, similar to WT OPCs, HMB treatment markedly upregulated PLP (Figure 5b,e) while decreasing the level of A2B5 (Figure 5b,f) in PPARβ$^{-/-}$ OPCs, indicating that HMB does not require PPARβ for maturation of OPCs.

To further confirm this finding, we examined the mRNA expression of different myelin-specific molecules by real-time PCR. Consistent with immunofluorescence results, HMB remained unable to upregulate the mRNA expression of *MBP* (Figure 6a), *PLP* (Figure 6c), *MOG* (Figure 6e), and *CNPase* (Figure 6g) in PPARα$^{-/-}$ OPCs. In contrast, HMB markedly increased the mRNA expression of *MBP* (Figure 6b), *PLP* (Figure 6d), *MOG* (Figure 6f), and *CNPase* (Figure 6h) in OPCs isolated from PPARβ$^{\beta}$ mice. Consistent

with immunofluorescence finding, HMB also decreased the mRNA expression of *NG2* in PPARβ$^{-/-}$ (Figure 6j), but not PPARα$^{-/-}$ (Figure 6i), OPCs.

Next, to investigate the role of PPARγ, we used GW9662, a specific inhibitor of PPARγ. Interestingly, GW9662 remained unable to inhibit the HMB-mediated increase in PLP^{+} cells (Figure 7a,b) and decrease in A2B5^{+} cells (Figure 7a,c) in WT OPCs. Consistently, GW9662 also could not modulate the HMB-mediated upregulation of *MBP* (Figure 7d) and *PLP* (Figure 7e) mRNAs in WT OPCs (Figure 7). To understand the specificity of this finding and to confirm the involvement of PPARα and PPARβ further, we used GW6471, a specific antagonist of PPARα, and GSK0660, an antagonist of PPARβ. In contrast to GW9662 and consistent with that observed in PPARα$^{-/-}$ OPCs, GW6471 strongly abrogated the ability of HMB to decrease NG2^{+} cells (Figure 8a,b) and increase MBP^{+} cells (Figure 8a,c) in WT OPCs. In contrast, similar to PPARγ antagonist GW9662, GSK0660 had no effect on an HMB-mediated decrease in NG2^{+} cells (Figure 8d,e) and an increase in MBP^{+} cells (Figure 8d,f) in WT OPCs. These results suggest that PPARα, but neither PPARβ nor PPARγ, is involved in HMB-induced maturation of OPCs.

4.5 | Do agonists of PPARα, PPARβ, and PPARγ stimulate the maturation of OPCs into oligodendrocytes?

Since HMB required PPARα, but neither PPARβ nor PPARγ, to stimulate the maturation of OPCs, we examined whether agonism of PPARα by a selective agonist was able to stimulate the maturation of OPCs into oligodendrocytes. Several studies have identified GW7647 as a potent agonist of PPARα (Patil et al., 2019; Qu et al., 2022). Treatment of WT OPCs with GW7647 for 24 h led to a robust decrease in NG2^{+} cells (Figure 9a,b) and an increase in MBP^{+} cells (Figure 9a,c). On the contrary, we did not find any decrease in NG2^{+} cells (Figure 9d,e,g,h) and increase in MBP^{+} cells (Figure 9d,f,g,i) with either PPARβ agonist GW0742 or PPARγ agonist GW1929. These results indicate that activation of PPARα by GW7647, but neither PPARβ by GW0742 nor PPARγ by GW1929, is capable of stimulating the maturation of OPCs into oligodendrocytes.

4.6 | HMB induces the recruitment of PPARα, but neither PPARβ nor PPARγ, to the promoter of *PLP* gene in WT OPCs

Next, to describe whether PPARα was directly involved in the transcription of myelin-associated genes in HMB-treated OPCs, we employed a ChIP assay to examine the recruitment of PPARα to *PLP* gene promoter. Figure 10a describes the presence of a consensus PPRE in the proximal region of the *PLP* gene promoter. We used antibodies against PPARα, PPARβ, PPARγ, CBP, and RNA polymerase to prepare immunoprecipitates from chromatin fragments of HMB-treated OPCs. From PCR of immunoprecipitates, we were also able to amplify 170 bp fragment of the *PLP* promoter corresponding to the PPRE (Figure 10a) when antibodies against PPARα were used for immunoprecipitation (PCR, Figure 10b; real-time PCR, Figure 10c). On the contrary, from immunoprecipitates of HMB-treated OPCs with antibodies against either PPARβ (Figure 10b,d) or PPARγ (Figure 10b,e), we could not amplify 170 bp fragment of the *PLP* promoter. These results suggest that HMB specifically induces the recruitment of PPARα, but neither PPARβ nor PPARγ, to the PPRE of the PLP gene promoter in OPCs.

CREB-binding protein (CBP) is one of the key histone acetyltransferases that is known to play an important role in the transcription of genes associated with neuroprotection (Saha et al., 2007; Saha & Pahan, 2006). As obvious from PCR (Figure 10b) and real-time PCR (Figure 10f), HMB treatment of OPCs led to strong employment of CBP to the *PLP* gene promoter. Consistently, similar to the enrolment of CBP to the PPRE, HMB stimulation was also able to recruit RNA polymerase to the *PLP* gene promoter (Figure 10b,g). These results are specific since we did not observe any amplification product from the immunoprecipitates obtained with control IgG (Figure 10b,h). Taken together, these findings indicate that the HMB-induced transcriptional complex at the *PLP* promoter in OPCs contains PPARα, CBP, and RNA polymerase (Figure 10i).

4.7 | While OPCs in vivo in the brain of EAE mice express PPARα, but not PPARβ, the level of PPARβ, but not PPARα, is decreased in the brain of EAE mice

EAE serves as an animal model of MS (Baxter, 2007; Mondal et al., 2020). Although HMB requires PPARα, but not PPARβ, to stimulate the maturation of OPCs into oligodendrocytes, recently we have seen that oral HMB treatment protects mice from EAE via PPARβ, but not PPARα (Sheinin et al., 2023). To understand the basis of this dichotomy, MOG35-55-induced EAE mice were treated with HMB (5 mg/kg body wt/day) via gavage from 10 dpi for 10 d followed by double-labeling of cortical sections with antibodies against NG2 and PPARα/PPARβ. As expected, the number of NG2-positive cells increased markedly in the cortex of EAE mice in comparison to control mice (Figure S3A-C). Similar to that found in cultured OPCs, oral HMB treatment reduced the number of NG2-positive cells in the cortex of EAE mice (Figure S3A-C). Double-label immunofluorescence analysis showed that NG2-positive cells in the cortex of EAE mice expressed PPARα (Figure S3A), but not PPARβ (Figure S3B). Interestingly, the level of PPARα did not decrease in the cortex of EAE mice as compared to control mice and HMB treatment also did not increase the level of PPARα further in EAE mice (Figure S3A,D). In contrast, induction of EAE reduced the level of PPARβ in the cortex of EAE mice as compared to control mice and oral administration of HMB upregulated the level of PPARβ in EAE mice (Figure S3B,E), indicating a possible reason behind the involvement of PPARβ, but not PPARα, in HMB-mediated protection of EAE mice.

5 | DISCUSSION

Increasing the maturation of OPCs to mature oligodendrocytes is key to the remyelination of demyelinated axons in demyelinating disorders like MS, PML, etc. (Kuhn et al., 2019; Tepavcevic & Lubetzki, 2022). Therefore, it is important to delineate molecular mechanisms by which OPCs could be switched to mature oligodendrocytes and how such cellular processes could be modulated by a safe and effective drug to achieve remyelination.

HMB is a popular nutritional supplement among the health and fitness community for its potential to positively modulate exercise routine and muscle growth. In addition to helping the body-building community, HMB intake is known to improve protein balance and reduce muscle wasting in cancer (Molfino et al., 2013), acquired immunodeficiency syndrome (AIDS) (Clark et al., 2000), and aging (Vukovich, Stubbs, & Bohlken, 2001). It

has been also demonstrated that HMB supplementation results in a net reduction in total cholesterol (5.8%, $p < 0.03$), a decrease in LDL cholesterol (7.3%, $p < 0.01$), and a lessening in systolic blood pressure (4.4mm Hg, $p < 0.05$) compared with the placebo (Nissen et al., 2000). It is readily available from health food centers, supplement stores, and online. Nissen et al. (2000) have reported that HMB can be taken safely as an ergogenic aid for exercise. According to Vukovich et al, the plasma half-life of HMB is approximately 2.5 h and 9 h after ingestion plasma HMB reaches the baseline levels (Vukovich, Slater, et al., 2001). Here, we report for the first time that HMB is capable of switching OPCs into oligodendrocytes. Our results suggest the possible use of this easily available muscle-building supplement for remyelination in demyelinating disorders.

Mechanisms by which HMB converts OPCs into oligodendrocytes are not known. Although peroxisome proliferator-activated receptors (PPARs) (Alex et al., 2013; Georgiadi & Kersten, 2012), a nuclear hormone receptor family of transcription factors, are known to control the metabolism of lipids (Pahan, 2006; Roy & Pahan, 2015), several studies have reported an important role of PPARβ in myelination (Jana et al., 2012; Saluja et al., 2001). Since HMB is a derivative of butyric acid, a short-chain fatty acid (SCFA), which is known to activate PPARs, we examined the role of PPARs in HMB-driven switching of OPCs into oligodendrocytes. However, HMB induced the activation of PPRE-driven luciferase activity in astrocytes isolated from PPARβ$^{-/-}$, but not PPARα$^{-/-}$, mice, indicating the involvement of PPARα in HMB-induced upregulation of PPRE-luciferase. Similarly, HMB treatment led to nuclear localization of PPARα, but not PPARβ, in OPCs. These results also indicate the activation of PPARα by HMB. Consistently, HMB remained unable to drive the switching of PPARα$^{-/-}$ OPCs into oligodendrocytes, and HMB readily converted PPARβ$^{-/-}$ OPCs into oligodendrocytes. Therefore, although HMB required PPARβ to suppress EAE in mice (Sheinin et al., 2023), it employed PPARα to drive the differentiation of OPCs to oligodendrocytes. While induction of EAE reduced the level of PPARβ drastically in the cortex of EAE mice, PPARα remained unaffected. Moreover, HMB treatment increased and/or restored PPARβ in the cortex of EAE mice, without modulating the level of PPARα. It appears that PPARβ, but not PPARα, is sensitive to the EAE disease process, and thereby, HMB involves PPARβ, but not PPARα, for neuroprotection in EAE mice. Here, we must mention that in addition to PPARα, our in silico analysis has also identified the interaction of HMB with the LBD of PPARβ.

According to Zhang et al., the beneficial effect of IL-4 on oligodendrocyte differentiation is mediated by the PPARγ (Zhang et al., 2019). However, in our study, GW9662, a specific inhibitor of PPARγ, does not inhibit/modulate HMB-driven maturation of OPCs into oligodendrocytes, suggesting that PPARγ is not involved here. Although PPARβ plays an important role in myelination (Jana et al., 2012), these results suggest the involvement of PPARα, but not PPARβ, in HMB-induced switching of OPCs into oligodendrocytes. Moreover, PPARα plays an important role in the β-oxidation of fatty acids and fatty acid β-oxidation has also been reported in astrocytes in the CNS (Morita et al., 2012; Pahan, 2006). Therefore, there may be a crosstalk between fatty acid β-oxidation and maturation of OPCs that may be elucidated in further studies.

How does PPARα control the switching of OPCs? While OPCs are characterized by NG2 and A2B5, classical markers of oligodendrocytes are PLP, MBP, and MOG (Dincman et al., 2012; Domanska-Janik et al., 1997; Jana & Pahan, 2005, 2007). Upon analysis of promoters of these OPC-and oligodendrocyte-associated genes, we have seen that one or more PPRE is present in the promoters of *MBP*, *PLP*, and *MOG* genes. In contrast, we did not find any PPRE in the promoter of *NG2* and *A2B5* genes. Recruitment of transcription factors to the promoter of a particular gene is important for the transcription of that gene. Upon ChIP analysis of the *PLP* gene promoter, we have seen the recruitment of PPARα, but neither PPARβ nor PPARγ, to the PPRE by HMB treatment of OPCs, indicating the involvement of PPARα, but not the other two isoforms, in HMB-induced transcription of the *PLP* gene. Histone acetyltransferases (HATs) play an important role in keeping the chromatin in an open state via acetylation of histone (Saha et al., 2009; Saha & Pahan, 2006). The p300 and CBP (CREB-binding protein) are the two most important HATs (Saha et al., 2009; Saha & Pahan, 2006; Tyteca et al., 2006). However, HMB employed CBP, but not p300, to the *PLP* promoter in OPCs. Since HMB also induces the recruitment of RNA polymerase II to the same PPRE of *PLP* promoter, our results suggest that HMB employs the PPARα-CBP pathway for the transcription of myelin genes in OPCs to ultimately drive the differentiation of OPCs to oligodendrocytes.

Upon screening a G-protein-coupled receptor small-molecule library, Mei et al. have found that a number of κ-opioid receptor agonists are capable of promoting oligodendrocyte differentiation and myelination (Mei et al., 2016). According to Lairson and colleagues (Beyer et al., 2018), taurine, an aminosulfonic acid, enhances OPC differentiation and maturation. Although there are some experimental drugs to stimulate remyelination, HMB has established itself as a safe supplement. Many athletes and body-builders have been taking HMB for years on a daily basis without any known side effects. Different clinical trials (Clark et al., 2000; Kuhls et al., 2007; May et al., 2002; Rahimi et al., 2018; Sanchez-Martinez et al., 2018) also did not notice any untoward effect of HMB. Therefore, HMB may have advantages over other prospective drugs with respect to safety issues. In summary, here, we describe that HMB stimulates the differentiation of OPCs to mature oligodendrocytes via PPARα, highlighting an important possibility of taking care of remyelination with this body-building supplement.

Supplementary Material

Refer to Web version on PubMed Central for supplementary material.

ACKNOWLEDGEMENT

All experiments were conducted in compliance with the ARRIVE guidelines.

FUNDING INFORMATION

This study was supported by a grant (AT10980) from NIH. Moreover, Dr. Pahan is the recipient of a Research Career Scientist Award (1IK6 BX004982) from the Department of Veterans Affairs. However, the views expressed in this article are those of the authors and do not necessarily reflect the position or policy of the Department of Veterans Affairs or the United States government.

U.S. Department of Veterans Affairs, Grant/Award Number: 1IK6 BX004982; Center for Information Technology, Grant/Award Number: AT10980

DATA AVAILABILITY STATEMENT

The data that support the findings of this study are available from the corresponding author upon reasonable request.

Abbreviations:

ChIP	chromatin immunoprecipitation
CNPase	2′,3′-cyclic nucleotide 3′-phosphohydrolase
dpi	days post-immunization
EAE	experimental autoimmune encephalomyelitis
GAPDH	glyceraldehyde 3-phosphate dehydrogenase
HMB	β-hydroxy β-methylbutyrate
LBD	ligand-binding domain
MBP	myelin basic protein
MOG	myelin oligodendrocyte glycoprotein
MS	multiple sclerosis
NG2	neural/glial antigen 2
OPCs	oligodendroglial progenitor cells
PLP	proteolipid protein
PPAR	peroxisome proliferator-activated receptor
PPRE	peroxisome proliferator-responsive element
RRID	research resource identifier
S280A	serine 280 alanine
Y314	tyrosine 314
Y464	tyrosine 464

REFERENCES

Akassoglou K, Bauer J, Kassiotis G, Pasparakis M, Lassmann H, Kollias G, & Probert L (1998). Oligodendrocyte apoptosis and primary demyelination induced by local TNF/p55TNF receptor signaling in the central nervous system of transgenic mice: Models for multiple sclerosis with primary oligodendrogliopathy. The American Journal of Pathology, 153, 801–813. [PubMed: 9736029]

Alex S, Lange K, Amolo T, Grinstead JS, Haakonsson AK, Szalowska E, Koppen A, Mudde K, Haenen D, al-Lahham S', Roelofsen H, Houtman R, van der Burg B, Mandrup S, Bonvin AMJJ, Kalkhoven E, Müller M, Hooiveld GJ, & Kersten S (2013). Short-chain fatty acids stimulate angiopoietin-like 4 synthesis in human colon adenocarcinoma cells by activating peroxisome proliferator-activated receptor gamma. Molecular and Cellular Biology, 33, 1303–1316. [PubMed: 23339868]

Baxter AG (2007). The origin and application of experimental autoimmune encephalomyelitis. Nature Reviews. Immunology, 7, 904–912.

Beyer BA, Fang M, Sadrian B, Montenegro-Burke JR, Plaisted WC, Kok BPC, Saez E, Kondo T, Siuzdak G, & Lairson LL (2018). Metabolomics-based discovery of a metabolite that enhances oligodendrocyte maturation. Nature Chemical Biology, 14, 22–28. [PubMed: 29131145]

Brahmachari S, & Pahan K (2007). Sodium benzoate, a food additive and a metabolite of cinnamon, modifies T cells at multiple steps and inhibits adoptive transfer of experimental allergic encephalomyelitis. Journal of Immunology, 179, 275–283.

Caprariello AV, Mangla S, Miller RH, & Selkirk SM (2012). Apoptosis of oligodendrocytes in the central nervous system results in rapid focal demyelination. Annals of Neurology, 72,395–405. [PubMed: 23034912]

Chandra G, Roy A, Rangasamy SB, & Pahan K (2017). Induction of adaptive immunity leads to nigrostriatal disease progression in MPTP mouse model of Parkinson's disease. Journal of Immunology, 198, 4312–4326.

Chandra S, Jana M, & Pahan K (2018). Aspirin induces lysosomal biogenesis and attenuates amyloid plaque pathology in a mouse model of Alzheimer's disease via PPARalpha. The Journal of Neuroscience, 38, 6682–6699. [PubMed: 29967008]

Clark RH, Feleke G, Din M, Yasmin T, Singh G, Khan FA, & Rathmacher JA (2000). Nutritional treatment for acquired immunodeficiency virus-associated wasting using beta-hydroxy beta-methylbutyrate, glutamine, and arginine: A randomized, double-blind, placebo-controlled study. JPEN Journal of Parenteral and Enteral Nutrition, 24, 133–139. [PubMed: 10850936]

Corbett GT, Gonzalez FJ, & Pahan K (2015). Activation of peroxisome proliferator-activated receptor alpha stimulates ADAM10-mediated proteolysis of APP. Proceedings of the National Academy of Sciences of the United States of America, 112, 8445–8450. [PubMed: 26080426]

Dasgupta S, Jana M, Zhou Y, Fung YK, Ghosh S, & Pahan K (2004). Antineuroinflammatory effect of NF-kappaB essential modifier-binding domain peptides in the adoptive transfer model of experimental allergic encephalomyelitis. Journal of Immunology, 173, 1344–1354.

Dasgupta S, Zhou Y, Jana M, Banik NL, & Pahan K (2003). Sodium phenylacetate inhibits adoptive transfer of experimental allergic encephalomyelitis in SJL/J mice at multiple steps. Journal of Immunology, 170, 3874–3882.

Dincman TA, Beare JE, Ohri SS, & Whittemore SR (2012). Isolation of cortical mouse oligodendrocyte precursor cells. Journal of Neuroscience Methods, 209, 219–226. [PubMed: 22743801]

Domanska-Janik K, Sypecka J, & Taraszewska A (1997). Immunohistochemical study of myelin-specific proteins in pt rabbits. Folia Neuropathologica, 35, 1–7. [PubMed: 9161094]

Durkalec-Michalski K, Jeszka J, & Podgorski T (2017). The effect of a 12-week beta-hydroxy-beta-methylbutyrate (HMB) supplementation on highly-trained combat sports athletes: A randomised, double-blind, placebo-controlled crossover study. Nutrients, 9, 753. [PubMed: 28708126]

Dutta D, Jana M, Majumder M, Mondal S, Roy A, & Pahan K (2021). Selective targeting of the TLR2/MyD88/NF-kappaB pathway reduces alpha-synuclein spreading in vitro and in vivo. Nature Communications, 12, 5382.

Dutta D, Paidi RK, Raha S, Roy A, Chandra S, & Pahan K (2022). Treadmill exercise reduces alpha-synuclein spreading via PPARalpha. Cell Reports, 40, 111058. [PubMed: 35830804]

Figarella-Branger D, Colin C, Baeza-Kallee N, & Tchoghandjian A (2022). A2B5 expression in central nervous system and gliomas. International Journal of Molecular Sciences, 23, 4670. 10.3390/ijms23094670 [PubMed: 35563061]

Friese MA, Schattling B, & Fugger L (2014). Mechanisms of neurodegeneration and axonal dysfunction in multiple sclerosis. Nature Reviews. Neurology, 10, 225–238. [PubMed: 24638138]

Georgiadi A, & Kersten S (2012). Mechanisms of gene regulation by fatty acids. Advances in Nutrition, 3, 127–134. [PubMed: 22516720]

Ghosh A, Roy A, Liu X, Kordower JH, Mufson EJ, Hartley DM, Ghosh S, Mosley RL, Gendelman HE, & Pahan K (2007). Selective inhibition of NF-kappaB activation prevents dopaminergic neuronal loss in a mouse model of Parkinson's disease. Proceedings of the National Academy of Sciences of the United States of America, 104, 18754–18759. [PubMed: 18000063]

Ghosh A, Roy A, Matras J, Brahmachari S, Gendelman HE, & Pahan K (2009). Simvastatin inhibits the activation of p21ras and prevents the loss of dopaminergic neurons in a mouse model of Parkinson's disease. The Journal of Neuroscience, 29, 13543–13556. [PubMed: 19864567]

Gottschalk CG, Jana M, Roy A, Patel DR, & Pahan K (2021). Gemfibrozil protects dopaminergic neurons in a mouse model of Parkinson's disease via PPARalpha-dependent astrocytic GDNF pathway. The Journal of Neuroscience, 41, 2287–2300. [PubMed: 33514677]

Hartline DK (2008). What is myelin? Neuron Glia Biology, 4, 153–163. [PubMed: 19737435]

Jana A, Hogan EL, & Pahan K (2009). Ceramide and neurodegeneration: Susceptibility of neurons and oligodendrocytes to cell damage and death. Journal of the Neurological Sciences, 278, 5–15. [PubMed: 19147160]

Jana A, Modi KK, Roy A, Anderson JA, van Breemen RB, & Pahan K (2013). Up-regulation of neurotrophic factors by cinnamon and its metabolite sodium benzoate: Therapeutic implications for neurodegenerative disorders. Journal of Neuroimmune Pharmacology, 8, 739–755. [PubMed: 23475543]

Jana A, & Pahan K (2007). Oxidative stress kills human primary oligodendrocytes via neutral sphingomyelinase: Implications for multiple sclerosis. Journal of Neuroimmune Pharmacology, 2, 184–193. [PubMed: 18040843]

Jana M, Dasarathy S, Ghosh S, & Pahan K (2023). Upregulation of DJ-1 in dopaminergic neurons by a physically-modified saline: Implications for Parkinson's disease. International Journal of Molecular Sciences, 24, 4652. 10.3390/ijms24054652 [PubMed: 36902085]

Jana M, Dutta D, Poddar J, & Pahan K (2023). Activation of PPARalpha exhibits therapeutic efficacy in a mouse model of juvenile neuronal ceroid lipofuscinosis. The Journal of Neuroscience, 43, 1814–1829. [PubMed: 36697260]

Jana M, Jana A, Pal U, & Pahan K (2007). A simplified method for isolating highly purified neurons, oligodendrocytes, astrocytes, and microglia from the same human fetal brain tissue. Neurochemical Research, 32, 2015–2022. [PubMed: 17447141]

Jana M, Mondal S, Gonzalez FJ, & Pahan K (2012). Gemfibrozil, a lipid-lowering drug, increases myelin genes in human oligodendrocytes via peroxisome proliferator-activated receptor-beta. The Journal of Biological Chemistry, 287, 34134–34148. [PubMed: 22879602]

Jana M, & Pahan K (2005). Redox regulation of cytokine-mediated inhibition of myelin gene expression in human primary oligodendrocytes. Free Radical Biology & Medicine, 39, 823–831. [PubMed: 16109311]

Jana M, & Pahan K (2013). Down-regulation of myelin gene expression in human oligodendrocytes by nitric oxide: Implications for demyelination in multiple sclerosis. Journal of Clinical and Cellular Immunology, 4. 10.4172/2155-9899.1000157

Jarius S, & Wildemann B (2019). The history of neuromyelitis optica. Journal of Neuroinflammation, 10, 8.

Kirby L, Jin J, Cardona JG, Smith MD, Martin KA, Wang J, Strasburger H, Herbst L, Alexis M, Karnell J, Davidson T, Dutta R, Goverman J, Bergles D, & Calabresi PA (2019). Oligodendrocyte precursor cells present antigen and are cytotoxic targets in inflammatory demyelination. Nature Communications, 10, 3887.

Kondo Y, Adams JM, Vanier MT,& Duncan ID (2011). Macrophages counteract demyelination in a mouse model of globoid cell leukodystrophy. The Journal of Neuroscience, 31, 3610–3624. [PubMed: 21389217]

Kuhls DA, Rathmacher JA, Musngi MD, Frisch DA, Nielson J, Barber A, MacIntyre AD, Coates JE, & Fildes JJ (2007). Beta-hydroxy-beta-methylbutyrate supplementation in critically ill trauma patients. The Journal of Trauma, 62, 125–131; discussion 131–122. [PubMed: 17215743]

Kuhn S, Gritti L, Crooks D, & Dombrowski Y(2019). Oligodendrocytes in development, myelin generation and beyond. Cells, 8, 1424. 10.3390/cells8111424 [PubMed: 31726662]

Kundu M, Mondal S, Roy A, Martinson JL, & Pahan K (2016). Sodium benzoate, a food additive and a metabolite of cinnamon, enriches regulatory T cells via STAT6-mediated upregulation of TGF-beta. Journal of Immunology, 197, 3099–3110.

Kundu M, Roy A, & Pahan K (2017). Selective neutralization of IL-12 p40 monomer induces death in prostate cancer cells via IL-12-IFN-gamma. Proceedings of the National Academy of Sciences of the United States of America, 114, 11482–11487. [PubMed: 29073075]

May PE, Barber A, D'Olimpio JT, Hourihane A, & Abumrad NN (2002). Reversal of cancer-related wasting using oral supplementation with a combination of beta-hydroxy-beta-methylbutyrate, arginine, and glutamine. American Journal of Surgery, 183, 471–479. [PubMed: 11975938]

Mei F, Mayoral SR, Nobuta H, Wang F, Desponts C, Lorrain DS, Xiao L, Green AJ, Rowitch D, Whistler J, & Chan JR (2016). Identification of the kappa-opioid receptor as a therapeutic target for oligodendrocyte remyelination. The Journal of Neuroscience, 36, 7925–7935. [PubMed: 27466337]

Molfino A, Gioia G, Rossi Fanelli F, & Muscaritoli M (2013). Beta-hydroxy-beta-methylbutyrate supplementation in health and disease: A systematic review of randomized trials. Amino Acids, 45, 1273–1292. [PubMed: 24057808]

Mondal S, Dasarathi S, & Pahan K (2017). Glyceryl tribenzoate: A flavoring ingredient, inhibits the adoptive transfer of experimental allergic encephalomyelitis via TGF-beta: Implications for multiple sclerosis therapy. Journal of Clinical and Cellular Immunology, 8, 488. 10.4172/2155-9899.1000488 [PubMed: 28367355]

Mondal S, Jana M, Dasarathi S, Roy A, & Pahan K (2018). Aspirin ameliorates experimental autoimmune encephalomyelitis through interleukin-11-mediated protection of regulatory T cells. Science Signaling, 11, eaar8278. [PubMed: 30482850]

Mondal S, Kundu M, Jana M, Roy A, Rangasamy SB, Modi KK, Wallace J, Albalawi YA, Balabanov R, & Pahan K (2020). IL-12 p40 monomer is different from other IL-12 family members to selectively inhibit IL-12Rbeta1 internalization and suppress EAE. Proceedings of the National Academy of Sciences of the United States of America, 117, 21557–21567. [PubMed: 32817415]

Mondal S, Martinson JA, Ghosh S, Watson R, & Pahan K (2012). Protection of Tregs, suppression of Th1 and Th17 cells, and amelioration of experimental allergic encephalomyelitis by a physically-modified saline. PLoS ONE, 7, e51869. [PubMed: 23284794]

Mondal S, & Pahan K (2015). Cinnamon ameliorates experimental allergic encephalomyelitis in mice via regulatory T cells: Implications for multiple sclerosis therapy. PLoS ONE, 10, e0116566. [PubMed: 25569428]

Mondal S, Roy A, & Pahan K (2009). Functional blocking monoclonal antibodies against IL-12p40 homodimer inhibit adoptive transfer of experimental allergic encephalomyelitis. Journal of Immunology, 182, 5013–5023.

Morita M, Shinbo S, Asahi A, & Imanaka T (2012). Very long chain fatty acid beta-oxidation in astrocytes: Contribution of the ABCD1-dependentand -independent pathways. Biological & Pharmaceutical Bulletin, 35, 1972–1979. [PubMed: 23123468]

Nissen S, Sharp RL, Panton L, Vukovich M, Trappe S, & Fuller JC Jr. (2000). Beta-hydroxy-beta-methylbutyrate (HMB) supplementation in humans is safe and may decrease cardiovascular risk factors. The Journal of Nutrition, 130, 1937–1945. [PubMed: 10917905]

Pahan K. (2006). Lipid-lowering drugs. Cellular and Molecular Life Sciences, 63, 1165–1178. [PubMed: 16568248]

Pahan K, Jana M, Liu X, Taylor BS, Wood C, & Fischer SM (2002). Gemfibrozil, a lipid-lowering drug, inhibits the induction of nitric-oxide synthase in human astrocytes. The Journal of Biological Chemistry, 277, 45984–45991. [PubMed: 12244038]

Pahan K, Khan M, & Singh I (1998). Therapy for X-adrenoleukodystrophy: Normalization of very long chain fatty acids and inhibition of induction of cytokines by cAMP. Journal of Lipid Research, 39, 1091–1100. [PubMed: 9610777]

Pahan K, Liu X, McKinney MJ, Wood C, Sheikh FG, & Raymond JR (2000). Expression of a dominant-negative mutant of p21(ras) inhibits induction of nitric oxide synthase and activation

of nuclear factor-kappaB in primary astrocytes. Journal of Neurochemistry, 74, 2288–2295. [PubMed: 10820188]

Paidi RK, Jana M, Mishra RK, Dutta D, & Pahan K (2021). Selective inhibition of the interaction between SARS-CoV-2 spike SI and ACE2 by SPIDAR peptide induces anti-inflammatory therapeutic responses. Journal of Immunology, 207, 2521–2533.

Paidi RK, Jana M, Raha S, Mishra RK, Jeong B, Sheinin M, & Pahan K (2023). Prenol, but not vitamin C, of fruit binds to SARS-CoV-2 spike SI to inhibit viral entry: Implications for COVID-19. Journal of Immunology, 210, 1938–1949.

Paidi RK, Raha S, Roy A, & Pahan K (2023). Muscle-building supplement beta-hydroxy beta-methylbutyrate binds to PPARalpha to improve hippocampal functions in mice. Cell Reports, 42, 112717. [PubMed: 37437568]

Patel D, Roy A, Kundu M, Jana M, Luan CH, Gonzalez FJ, & Pahan K (2018). Aspirin binds to PPARα to stimulate hippocampal plasticity and protect memory. Proceedings of the National Academy of Sciences of the United States of America, 115, E7408–E7417. [PubMed: 30012602]

Patel D, Roy A, Raha S, Kundu M, Gonzalez FJ, & Pahan K (2020). Upregulation of BDNF and hippocampal functions by a hippocampal ligand of PPARalpha. JCI Insight, 5, e136654. 10.1172/jci.insight.136654 [PubMed: 32315292]

Patil R, Mohanty B, Liu B, Chandrashekaran IR, Headey SJ, Williams ML, Clements CS, Ilyichova O, Doak BC, Genissel P, Weaver RJ, Vuillard L, Halls ML, Porter CJH, & Scanlon MJ (2019). A ligand-induced structural change in fatty acid-binding protein 1 is associated with potentiation of peroxisome proliferator-activated receptor alpha agonists. The Journal of Biological Chemistry, 294, 3720–3734. [PubMed: 30598509]

Qu XX, He JH, Cui ZQ, Yang T, & Sun XH (2022). PPAR-alpha agonist GW7647 protects against oxidative stress and iron deposit via GPx4 in a transgenic mouse model of Alzheimer's diseases. ACS Chemical Neuroscience, 13, 207–216. [PubMed: 34965724]

Rahimi MH, Mohammadi H, Eshaghi H, Askari G, & Miraghajani M (2018). The effects of Beta-hydroxy-beta-methylbutyrate supplementation on recovery following exercise-induced muscle damage: A systematic review and meta-analysis. Journal of the American College of Nutrition, 37, 640–649. [PubMed: 29676656]

Rangasamy SB, Corbett GT, Roy A, Modi KK, Bennett DA, Mufson EJ, Ghosh S, & Pahan K (2015). Intranasal delivery of NEMO-binding domain peptide prevents memory loss in a mouse model of Alzheimer's disease. Journal of Alzheimer's Disease, 47, 385–402.

Richardson EP Jr. (1961). Progressive multifocal leukoencephalopathy. The New England Journal of Medicine, 265, 815–823. [PubMed: 14038684]

Roy A, Jana M, Kundu M, Corbett GT, Rangaswamy SB, Mishra RK, Luan CH, Gonzalez FJ, & Pahan K (2015). HMG-CoA reductase inhibitors bind to PPARalpha to upregulate Neurotrophin expression in the brain and improve memory in mice. Cell Metabolism, 22, 253–265. [PubMed: 26118928]

Roy A, Kundu M, Jana M, Mishra RK, Yung Y, Luan CH, Gonzalez FJ, & Pahan K (2016). Identification and characterization of PPARalpha ligands in the hippocampus. Nature Chemical Biology, 12, 1075–1083. [PubMed: 27748752]

Roy A, & Pahan K (2015). PPARalpha signaling in the hippocampus: Crosstalk between fat and memory. Journal of Neuroimmune Pharmacology, 10, 30–34. [PubMed: 25575492]

Saha RN, Ghosh A, Palencia CA, Fung YK, Dudek SM, & Pahan K (2009). TNF-alpha preconditioning protects neurons via neuron-specific up-regulation of CREB-binding protein. Journal of Immunology, 183, 2068–2078.

Saha RN, Jana M, & Pahan K (2007). MAPK p38 regulates transcriptional activity of NF-kappaB in primary human astrocytes via acetylation of p65. Journal of Immunology, 179, 7101–7109.

Saha RN, & Pahan K (2006). HATs and HDACs in neurodegeneration: A tale of disconcerted acetylation homeostasis. Cell Death and Differentiation, 13, 539–550. [PubMed: 16167067]

Sakry D, & Trotter J (2016). The role of the NG2 proteoglycan in OPC and CNS network function. Brain Research, 1638, 161–166. [PubMed: 26100334]

Saluja I, Granneman JG, & Skoff RP (2001). PPAR delta agonists stimulate oligodendrocyte differentiation in tissue culture. Glia, 33, 191–204. [PubMed: 11241737]

Sanchez-Martinez J, Santos-Lozano A, Garcia-Hermoso A, Sadarangani KP, & Cristi-Montero C (2018). Effects of beta-hydroxy-beta-methylbutyrate supplementation on strength and body composition in trained and competitive athletes: A metaanalysis of randomized controlled trials. Journal of Science and Medicine in Sport, 21, 727–735. [PubMed: 29249685]

Sanders FK, & Whitteridge D (1946). Conduction velocity and myelin thickness in regenerating nerve fibres. The Journal of Physiology, 105, 152–174.

Shan W, Palkar PS, Murray IA, McDevitt EI, Kennett MJ, Kang BH, Isom HC, Perdew GH, Gonzalez FJ, & Peters JM (2008). Ligand activation of peroxisome proliferator-activated receptor beta/delta (PPARbeta/delta) attenuates carbon tetrachloride hepatotoxicity by downregulating proinflammatory gene expression. Toxicological Sciences, 105, 418–428. [PubMed: 18622026]

Sheinin M, Mondal S, Roy A, Gorai S, Rangasamy SB, Poddar J, & Pahan K (2023). Suppression of experimental autoimmune encephalomyelitis in mice by beta-hydroxy beta-methylbutyrate, a body-building supplement in humans. Journal of Immunology, 211, 187–198.

Singh I, Pahan K, Khan M, & Singh AK (1998). Cytokine-mediated induction of ceramide production is redox-sensitive. Implications to proinflammatory cytokine-mediated apoptosis in demyelinating diseases. The Journal of Biological Chemistry, 273, 20354–20362. [PubMed: 9685387]

Smith T. (1921). The capsules or sheaths of bacillus actinoides. The Journal of Experimental Medicine, 34, 593–598. [PubMed: 19868580]

Tepavcevic V, & Lubetzki C (2022). Oligodendrocyte progenitor cell recruitment and remyelination in multiple sclerosis: The more, the merrier? Brain, 145, 4178–4192. [PubMed: 36093726]

Traka M, Podojil JR, McCarthy DP, Miller SD, & Popko B (2016). Oligodendrocyte death results in immune-mediated CNS demyelination. Nature Neuroscience, 19, 65–74. [PubMed: 26656646]

Tyteca S, Legube G, & Trouche D (2006). To die or not to die: A HAT trick. Molecular Cell, 24, 807–808. [PubMed: 17189182]

Vukovich MD, Slater G, Macchi MB, Turner MJ, Fallon K, Boston T, & Rathmacher J (2001). Beta-hydroxy-beta-methylbutyrate (HMB) kinetics and the influence of glucose ingestion in humans. The Journal of Nutritional Biochemistry, 12, 631–639. [PubMed: 12031256]

Vukovich MD, Stubbs NB, & Bohlken RM (2001). Body composition in 70-year-old adults responds to dietary beta-hydroxy-betamethylbutyrate similarly to that of young adults. The Journal of Nutrition, 131, 2049–2052. [PubMed: 11435528]

Zhang Q, Zhu W, Xu F, Dai X, Shi L, Cai W, Mu H, Hitchens TK, Foley LM, Liu X, Yu F, Chen J, Shi Y, Leak RK, Gao Y, Chen J, & Hu X (2019). The interleukin-4/PPARgamma signaling axis promotes oligodendrocyte differentiation and remyelination after brain injury. PLoS Biology, 17, e3000330. [PubMed: 31226122]

Zhu J, Eichler F, Biffi A, Duncan CN, Williams DA, & Majzoub JA (2020). The changing face of adrenoleukodystrophy. Endocrine Reviews, 41, 577–593. [PubMed: 32364223]

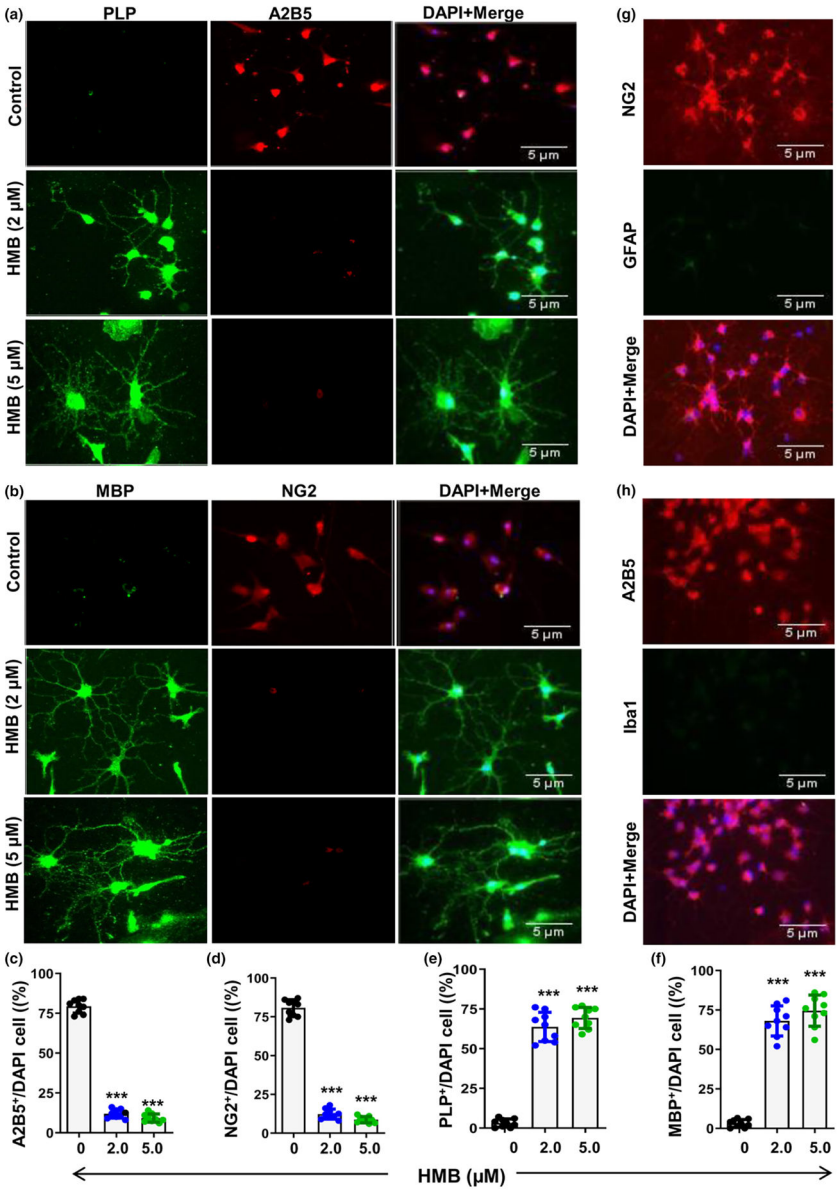

FIGURE 1.

Effect of β-hydroxy β-methylbutyrate (HMB) on the maturation of OPCs into OLs. (a) OPCs were treated with different concentrations (2 and 5 μM) of HMB for 48 h followed by double-labeling for PLP (red) and A2B5 (green). Nuclei were stained with DAPI (blue). (b) Similarly, cells were also double-labeled for NG2 (red) & MBP (green). Quantification of $A2B5^+$ (c), $NG2^+$ (d), PLP^+ (e), and MBP^+ (f) cells as a percentage of total cells ($DAPI^+$). Three fields per cell preparation from a total of three independent cell preparations per group were used for cell counting. Results are mean ± SEM. One-way ANOVA indicates [$F_{2,16}$ = 1468, $p < 0.0001$ (c); $F_{2,16}$ = 943.0, $p < 0.0001$ (d); $F_{2,16}$ = 232.3, $p < 0.0001$ (e); $F_{2,16}$ = 183.5, $p < 0.0001$ (f)]. A two-tailed paired *t*-test was also performed to test the significance of mean between control and HMB-treated groups. ***$p < 0.001$ versus control. To check

the purity of OPCs, cells were double-labeled for either NG2 & GFAP (g) or A2B5 & Iba1 (h). Results represent three independent cell preparations.

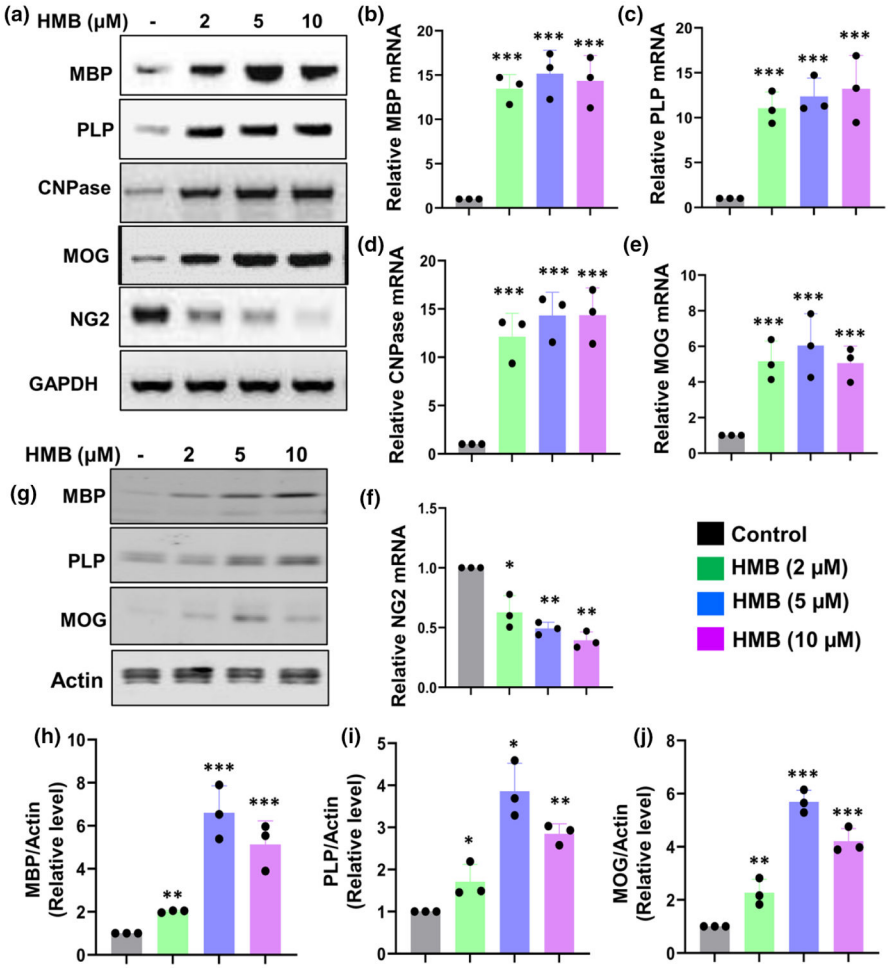

FIGURE 2.

Stimulation of myelin-specific genes by β-hydroxy β-methylbutyrate (HMB) in OPCs. OPCs were treated with different concentrations (2, 5, and 10 μM) of HMB for 5 h followed by monitoring the mRNA expression of MBP, PLP, CNPase, MOG, and NG2 by RT-PCR (a) and real-time PCR (MBP, b; PLP, c; CNPase, d; MOG, e; NG2, f). Results are mean ± SD of three different experiments. One-way ANOVA indicates [$F_{3,8} = 30.45$, $p = 0.0001$ (b); $F_{3,8} = 18.08$, $p = 0.0006$ (c); $F_{3,8} = 25.11$, $p = 0.0002$ (d); $F_{3,8} = 11.26$; $p = 0.0030$ (e); $F_{3,8} = 31.40$; $p < 0.0001$ (f)]. After 24 h of incubation with HMB, the protein level of MBP, PLP, and MOG was checked by Western blot (g). Actin was run as a loading control. Bands were scanned and values (H, MBP/Actin; I, PLP/Actin; J, MOG/Actin) presented as relative to control. Results are mean ± SD of three independent cell preparations. One-way ANOVA indicates [$F_{3,8} = 29.69$, $p = 0.0001$ (h); $F_{3,8} = 28.21$, $p = 0.0001$ (i); $F_{3,8} = 77.38$, $p < 0.0001$ (j)]. A two-tailed paired *t*-test was also performed to test the significance of mean between control and HMB-treated groups. *$p < 0.05$, **$p < 0.01$, & ***$p < 0.001$ versus control.

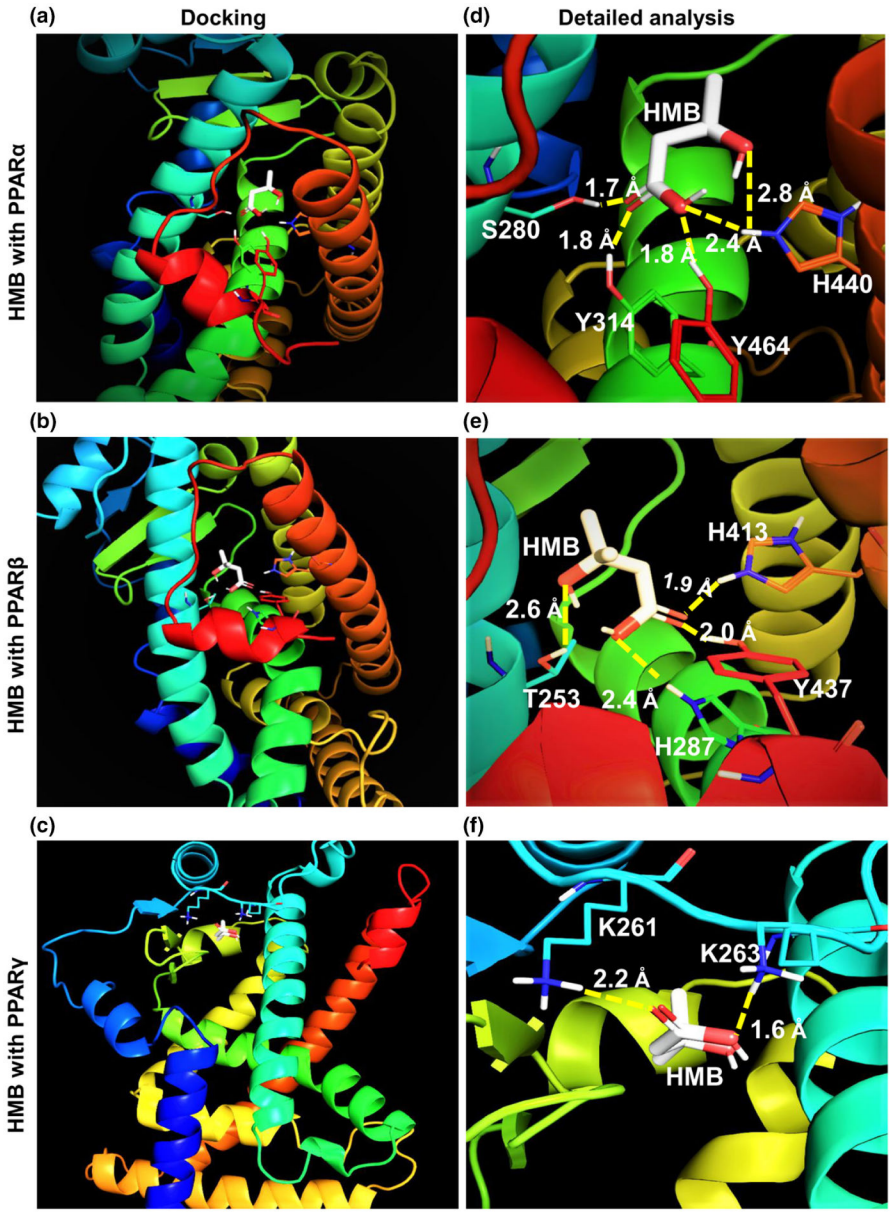

FIGURE 3.

In silico interaction analysis of β-hydroxy β-methylbutyrate (HMB) with PPARα, PPARβ, and PPARγ. (a) A rigid body in silico docked pose of HMB with PPARα (a), PPARβ (b), and PPARγ (c) was derived from the Autodock4. PyMOL software (The PyMol Molecular Graphics System, Version 2.0, Schrödinger, LLC.) was used to create the final representable image. A detailed view of PPARα (d), PPARβ (e), and PPARγ (f) was represented. HMB was found to be docked in the ligand-binding pocket of PPARα and PPARβ, but not PPARγ. The results represent three independent analyses.

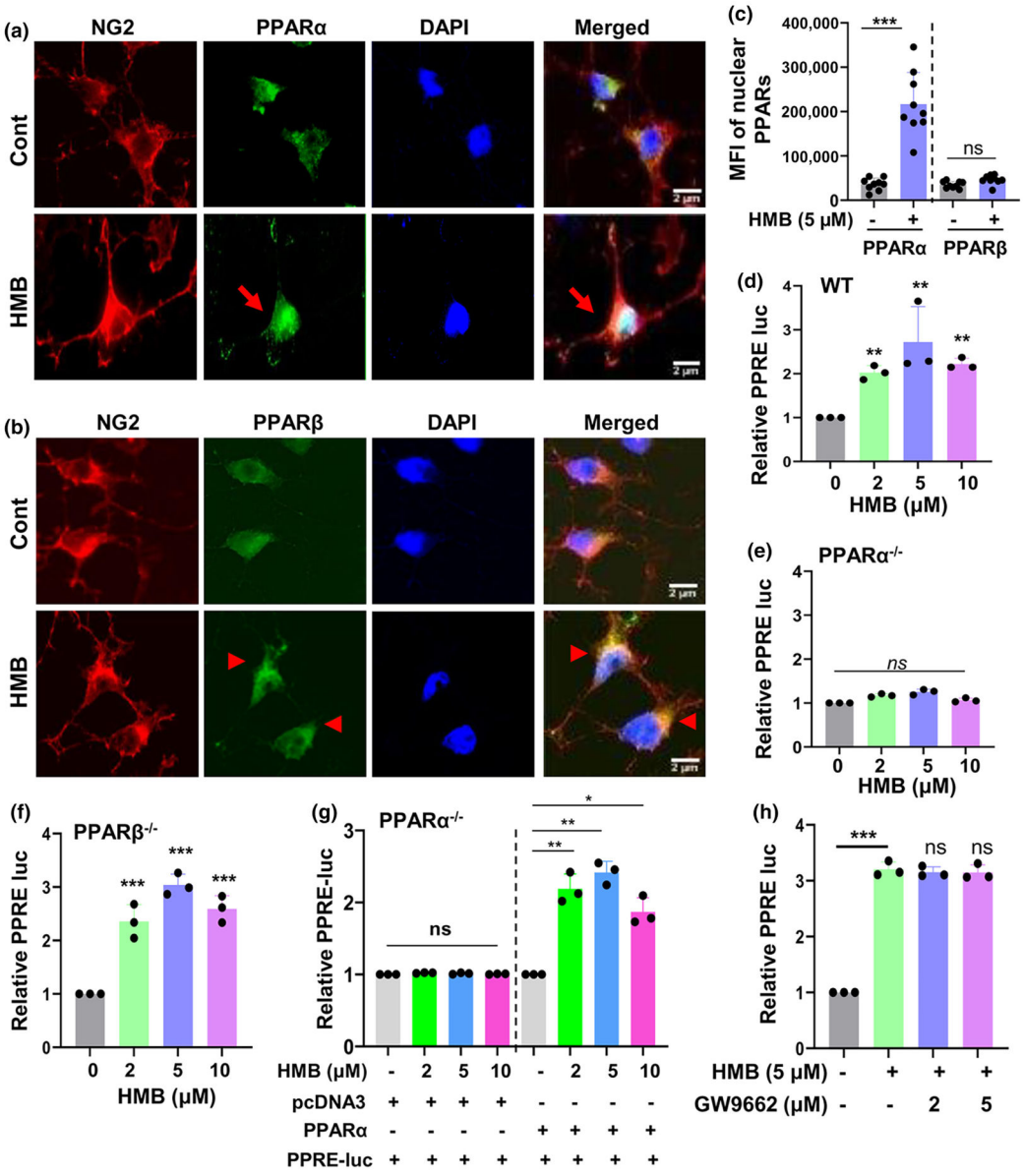

FIGURE 4.

β-hydroxy β-methylbutyrate (HMB) induces the activation of PPARα in OPCs and astrocytes. OPCs were treated with 5 μM HMB for 1 h followed by double-label immunofluorescence for NG2 & PPARα (a) and NG2 & PPARβ (b). Mean fluorescence intensity (MFI) of nuclear PPARα and PPARβ was quantified (c). Three fields per cell preparation from a total of three independent cell preparations per group were used for MFI quantification. A two-tailed paired *t*-test was performed to test the significance of mean between control and HMB-treated groups. ***$p < 0.001$ versus control; ns, not significant. Primary astrocytes isolated from WT (d), PPARα$^{-/-}$ (e), and PPARβ$^{-/-}$ (f) mice were transfected with tkPPREx3-Luc, a PPRE-dependent luciferase reporter construct. Twenty-four hours after transfection, cells were treated with different concentrations of HMB in serum-free media for 4 h followed by monitoring luciferase activity in total cell

extracts that is presented as relative to control. Results are mean ± SD of three independent cell preparations. A two-tailed paired *t*-test was performed to test the significance of mean between control and HMB-treated groups. $^{**}p < 0.01$ & $^{***}p < 0.001$ versus control; ns, not significant. (g) PPARα$^{-/-}$ astrocytes were transfected with tkPPREx3-Luc and either pcDNA3 (empty vector) or full-length PPARα cDNA. After 24 h, cells were treated with different concentrations of HMB for 4 h under serum-free conditions followed by measurement of luciferase activity in total cell extracts. (h) Twenty-four hours after transfection, WT astrocytes were treated with different concentrations of GW9662 for 1 h followed by stimulation with 5 μM HMB in serum-free media. After 4 h, luciferase activities were measured in cell lysates. Results are mean ± SD of three independent cell preparations. A two-tailed paired *t*-test was performed to test the significance of mean between control and HMB/GW9662-treated groups. $^{*}p < 0.05$, $^{**}p < 0.01$ & $^{***}p < 0.001$ versus control; ns, not significant.

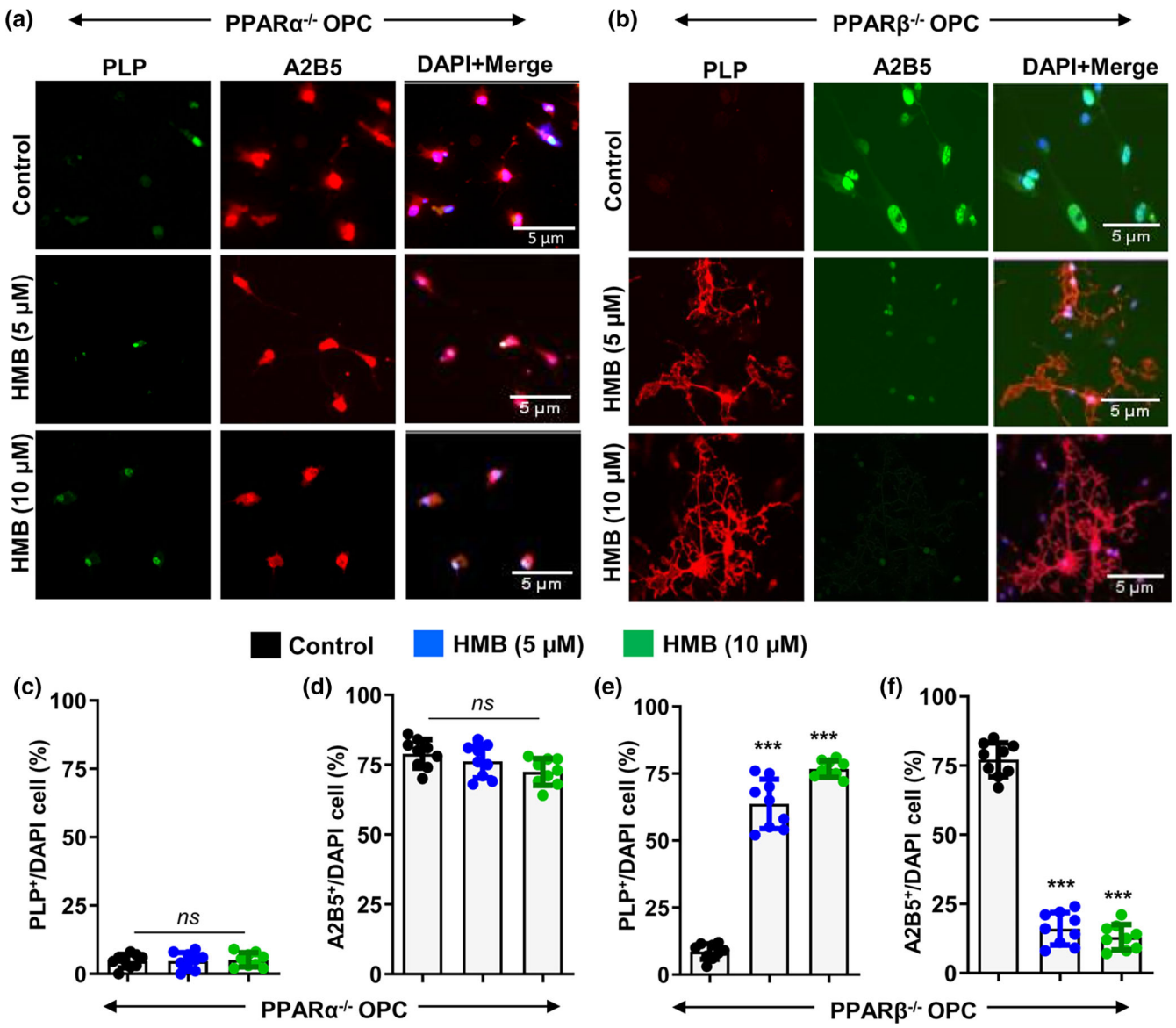

FIGURE 5.

β-hydroxy β-methylbutyrate (HMB) stimulates the maturation of OPCs into oligodendrocytes via PPARα, but not PPARβ. OPCs isolated from P1-P2 PPARα$^{-/-}$ and PPARβ$^{-/-}$ neonatal pups were treated with different concentrations of HMB. After 48 h of treatment, cells were double-labeled for PLP (green) and A2B5 (red) (a, PPARα$^{-/-}$ OPC; b, PPARβ$^{-/-}$ OPC). Nuclei were stained with DAPI (blue). Quantification of PLP^{+} (c, PPARα$^{-/-}$; e, PPARβ$^{-/-}$) and A2B5^{+} (d, PPARα$^{-/-}$; f, PPARβ$^{-/-}$) cells as a percentage of total cells (DAPI^{+}). Three fields per cell preparation from a total of three independent cell preparations per group were used for cell counting. Results are mean±SEM. One-way ANOVA indicates [$F_{2,24} = 0.08589$, $p = 0.9187$ (c); $F_{2,24} = 3.012$, $p < 0.0776$ (d); $F_{2,24} = 369.8$, $p < 0.0001$ (e); $F_{2,24} = 350.4$, $p < 0.0001$ (f)]. A two-tailed paired *t*-test was also performed to test the significance of mean between control and HMB-treated groups. ***$p <$ 0.001 versus control; ns, not significant.

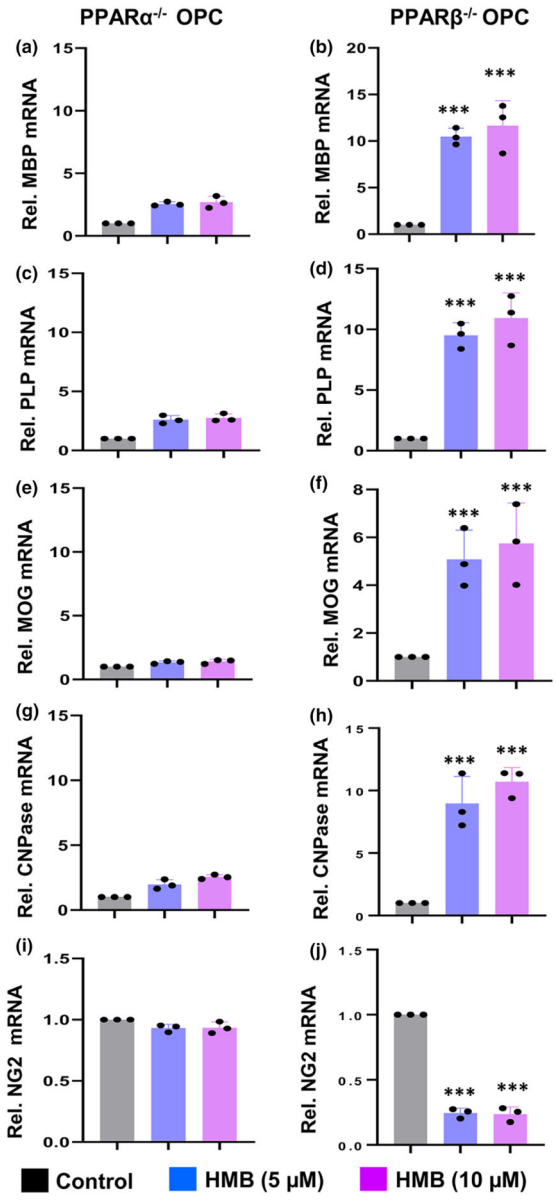

FIGURE 6.

β-hydroxy β-methylbutyrate (HMB) stimulates the expression of myelin-specific genes in OPCs mainly via PPARα, not PPARβ. OPCs isolated from P1-P2 PPARα$^{-/-}$ (a, c, e, g, & i) and PPARβ$^{-/-}$ (b, d, f, h, & j) neonatal pups were treated with different concentrations of HMB in the absence of FGF and PDGF. After 5 h of treatment, the mRNA expression of MBP (a & b), PLP (c & d), MOG (e & f), CNPase (g & h), and NG2 (i & j) was examined by real-time PCR. Results are mean±SD of three independent cell preparations. A two-tailed paired *t*-test was performed to test the significance of mean between control and HMB-treated groups. ***$p < 0.001$ versus control.

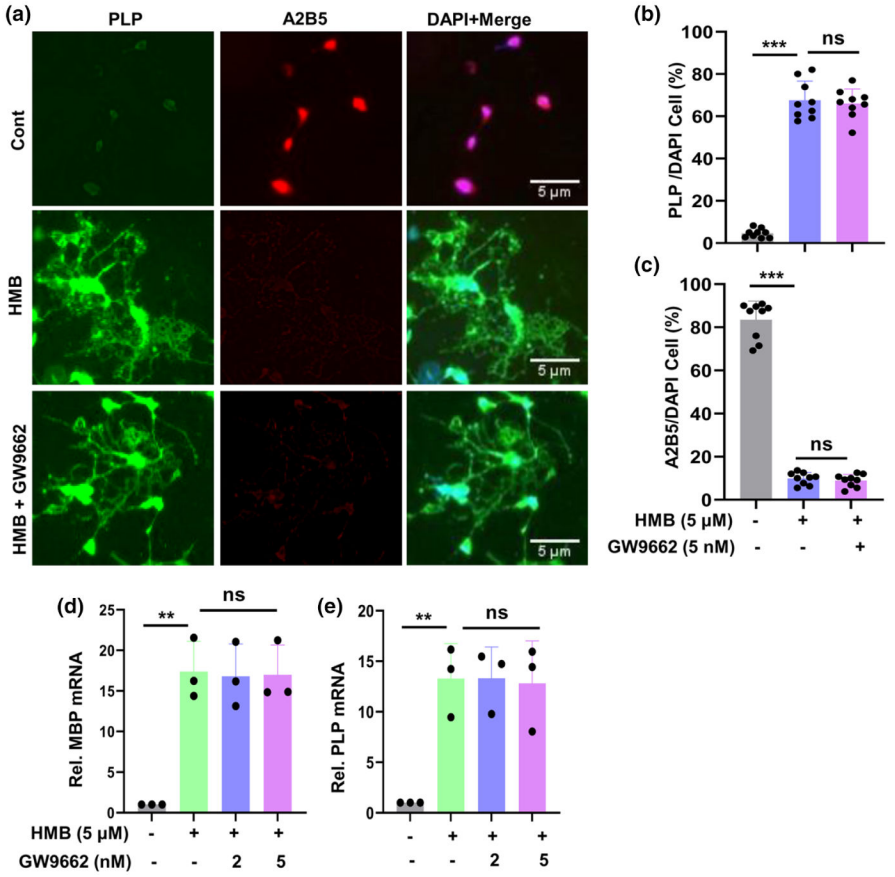

FIGURE 7.

Effect of GW9662 (an antagonist of PPARγ) on HMB-induced maturation of OPCs into oligodendrocytes. WT OPCs were treated with 5 nM GW9662 for 30 min followed by stimulation with 5 µM HMB. After 48 h of incubation, cells were double-labeled for PLP (green) and A2B5 (red) (a). Nuclei were stained with DAPI (blue). Quantification of PLP^+ (b) and $A2B5^+$ (c) cells as a percentage of total cells ($DAPI^+$). Three fields per cell preparation from a total of three independent cell preparations per group were used for cell counting. Results are mean ± SEM. ***$p < 0.001$; ns, not significant. After 5 h of HMB treatment, the mRNA expression of MBP (d) and PLP (e) was examined by real-time PCR. Results are mean ± SD of three independent cell preparations. A two-tailed paired *t*-test was performed to test the significance of mean between control and HMB/GW9662-treated groups. **$p < 0.01$ & ***$p < 0.001$ (b, control vs. HMB, $p < 0.0001$; c, control vs. HMB, $p < 0.0001$; d, control vs. HMB, $p = 0.0013$; e, control vs. HMB, $p = 0.0058$); ns, not significant (b, HMB vs. HMB + GW9662, $p = 0.8794$; c, HMB vs. HMB + GW9662, $p = 0.9262$; d, HMB vs. HMB + GW9662-2 nM, $p = 0.9959$ & HMB vs. HMB + GW9662-5 nM, $p = 0.9987$; e, HMB vs. HMB + GW9662-2 nM, $p = 0.9970$ & HMB vs. HMB + GW9662-5 nM, $p = 0.9975$).

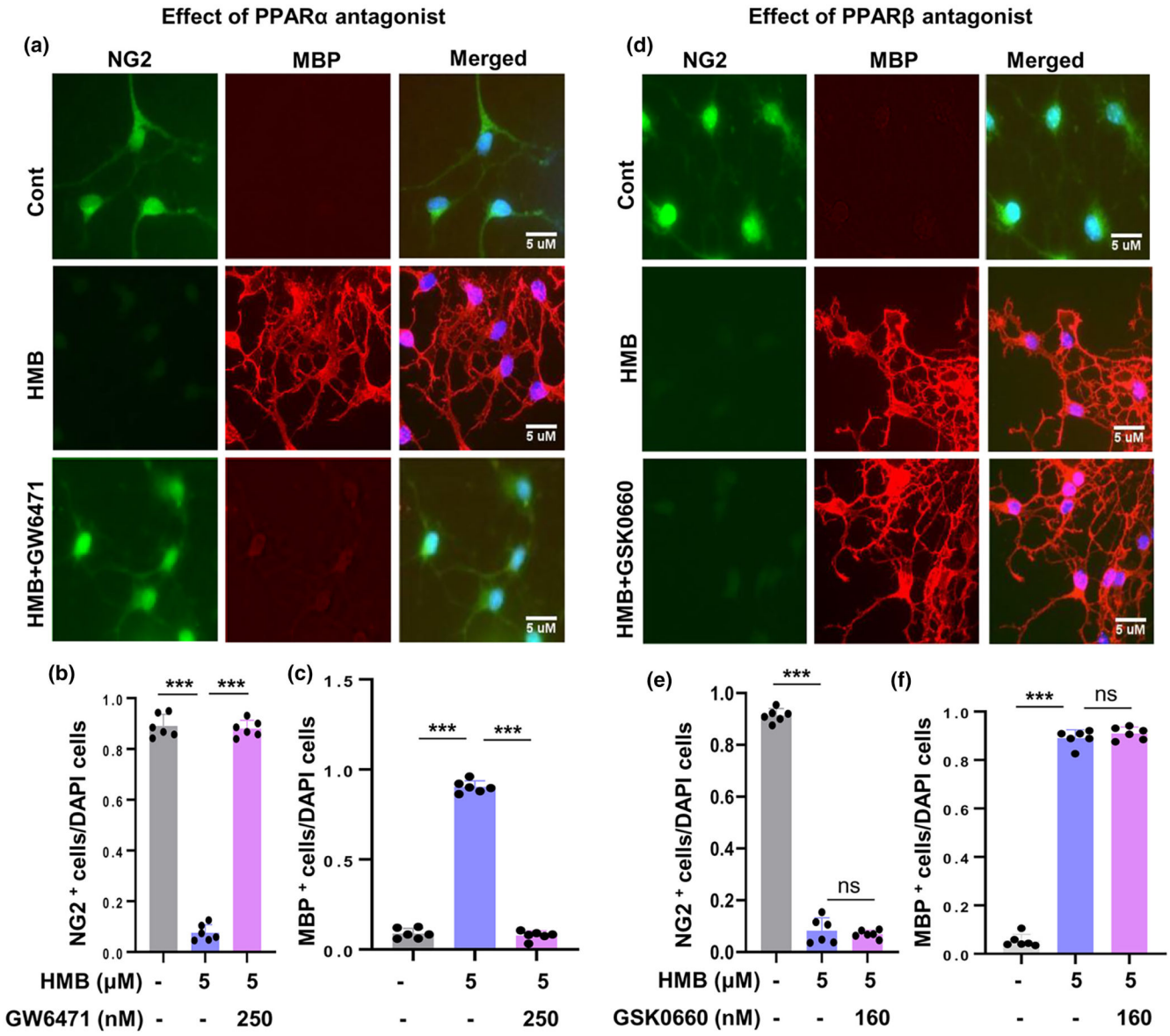

FIGURE 8.

Effect of GW6471 (an antagonist of PPARα) and GSK0660 (an antagonist of PPARβ) on HMB-induced maturation of OPCs into oligodendrocytes. WT OPCs were treated with 5 μM HMB in the presence or absence of 250 nM GW6471. After 48 h of treatment, cells were double-labeled for NG2 (green) and MBP (red) (a) followed by quantification of $NG2^+$ (b) and MBP^+ (c) cells with respect to total cells ($DAPI^+$). Similarly, OPCs were also treated with 5 μM HMB in the presence or absence of 160 nM GSK0660 for 48 h followed by double-labeling for NG2 and MBP (d) and quantification of $NG2^+$ (e) and MBP^+ (f) cells. Two fields per cell preparation from a total of three independent cell preparations per group were used for cell counting. Results are mean ± SEM. A two-tailed paired *t*-test was performed to test the significance of mean between control and either GW6471-treated groups (b & c) or GSK0660-treated groups (e & f). ***$p < 0.001$ (b, control vs. HMB, $p < 0.0001$ & HMB vs. HMB + GW6471, $p < 0.0001$; c, control vs. HMB, $p < 0.0001$ & HMB

vs. HMB + GW6471, $p < 0.0001$; e, control vs. HMB, $p < 0.0001$; f, control vs. HMB, $p < 0.0001$); ns, not significant (e, HMB vs. HMB + GSK0660, $p = 0.7939$; f, HMB vs. HMB + GSK0660, $p = 0.5010$).

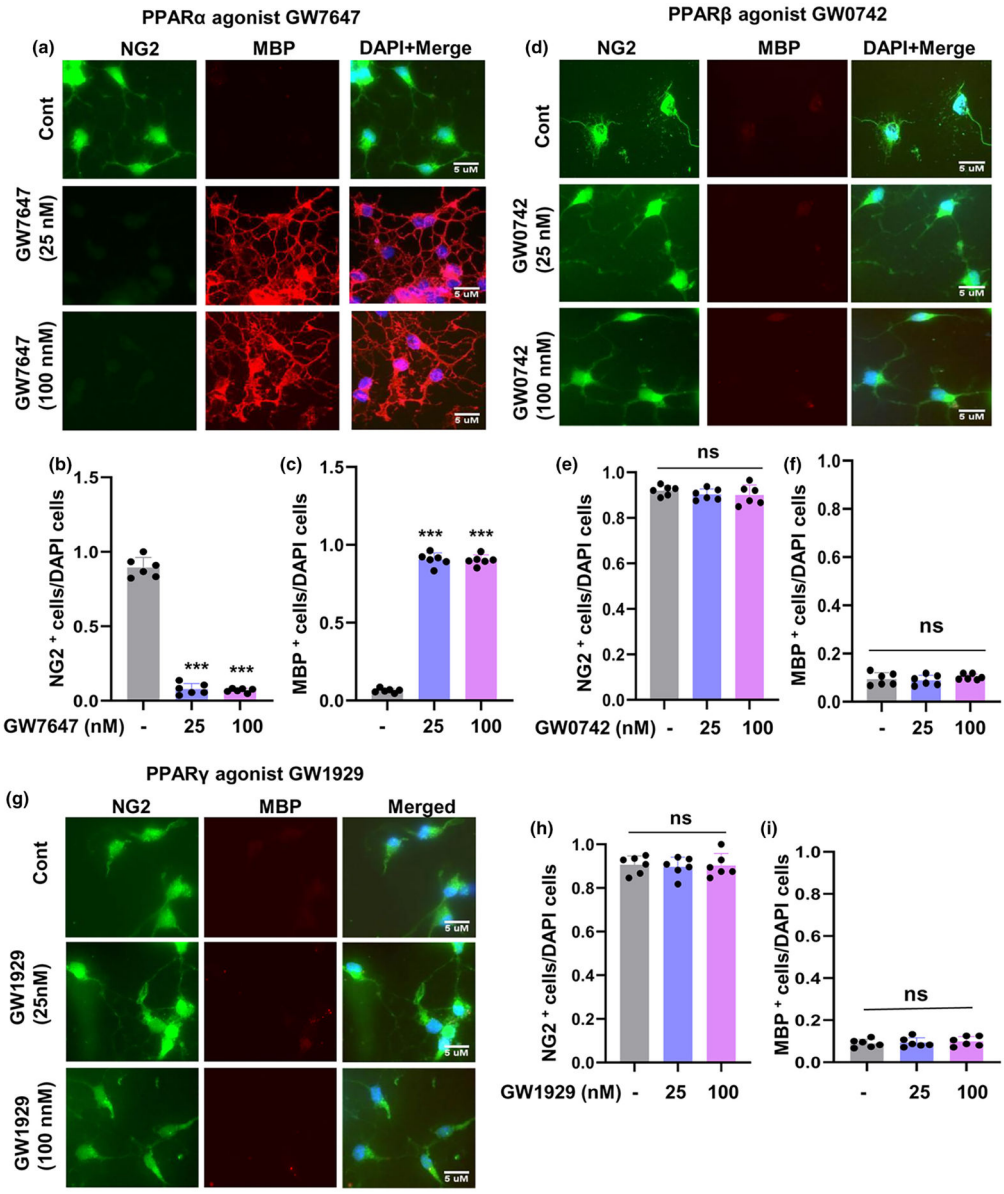

FIGURE 9.

Effect of agonists of PPARα (GW7647), PPARβ (GW0742), and PPARγ (GW1929) on the maturation of OPCs into oligodendrocytes. WT OPCs were treated with different concentrations of GW7647 (a–c), GW0742 (d–f), and GW1929 (g–i) for 48 h followed by double-labeling for NG2 and MBP (a, d & g) and quantification of $NG2^+$ (b, e & h) and MBP^+ (c, f & i) cells. Two fields per cell preparation from a total of three independent cell preparations per group were used for cell counting. Results are mean ± SEM. One-way ANOVA indicates [$F_{2,15} = 666.9$, $p < 0.0001$ (b); $F_{2,15} = 1352$, $p < 0.0001$ (c); $F_{2,15} = 0.6622$, $p = 0.5301$ (e); $F_{2,16} = 0.6748$, $p = 0.5241$ (f); $F_{2,15} = 0.06059$, $p = 0.9414$ (h); $F_{2,15} = 0.2615$, $p = 0.7733$ (i)]. A two-tailed paired *t*-test was also performed to test the significance of mean between control and GW7647-treated groups (b & c), GW0742-treated

groups (e & f), or GW1929-treated groups (h & i). ***$p < 0.001$ versus control; ns, not significant.

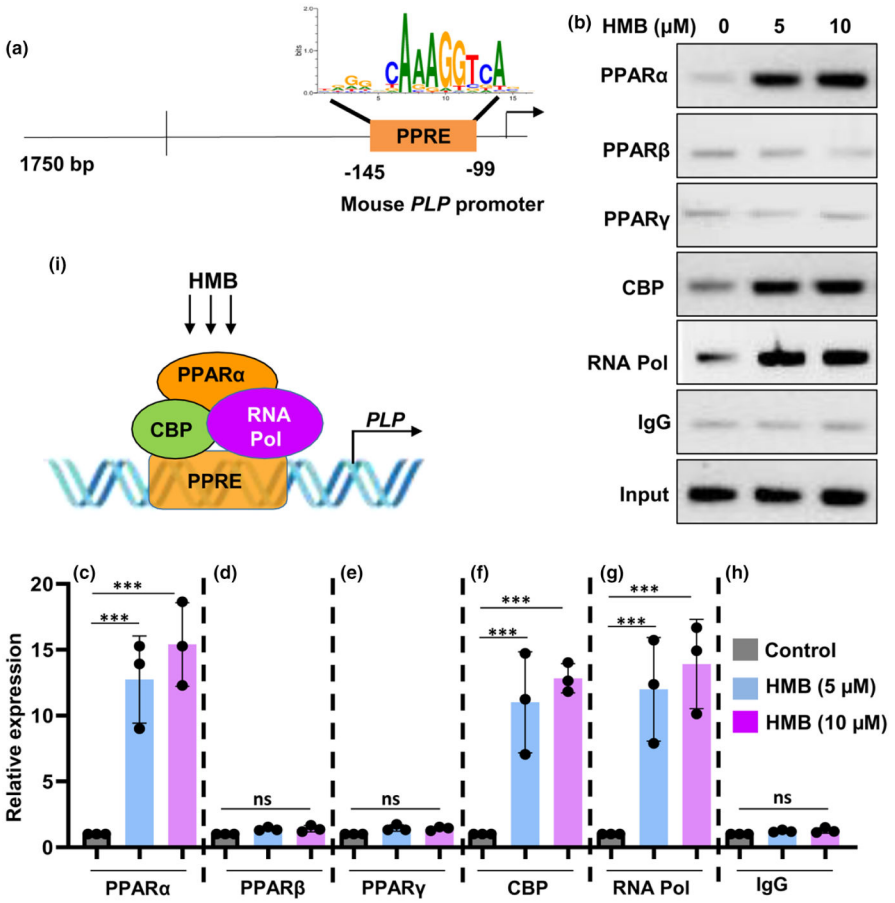

FIGURE 10.

β-hydroxy β-methylbutyrate (HMB) treatment stimulates the recruitment of PPARα, but neither PPARβ nor PPARγ, to the *PLP* gene promoter in WT OPCs. (a) Mouse *PLP* gene promoter harbors a consensus PPRE. OPCs were incubated with different concentrations of HMB for 1 h. Then immunoprecipitated chromatin fragments were amplified by semi-quantitative (b) and quantitative (c, PPARα; d, PPARβ; e, PPARγ; f, CBP; g, RNA polymerase; h, IgG) PCR as described under Section 2. Results are the mean ± SD of three independent cell preparations. ***$p < 0.001$; ns, not significant. Significance of mean between control and HMB-treated cells was analyzed by a two-tailed paired *t*-test. Here, we compared between control & 5 μM HMB and controls 10 μM HMB. (i) Schematic presentation of HMB-induced transcriptional activation of the *PLP* gene.